Soft Matter

REVIEW

View Article Online
View Journal | View Issue



Cite this: *Soft Matter*, 2022, **18**, 5535

# Progress in the self-assembly of organic/inorganic polyhedral oligomeric silsesquioxane (POSS) hybrids

Mohamed Gamal Mohamed and Shiao-Wei Kuo *

Received 16th May 2022,
Accepted 11th July 2022

DOI: 10.1039/d2sm00635a

rsc.li/soft-matter-journal

This Review describes recent progress in the self-assembly of organic/inorganic POSS hybrids derived from mono-, di-, and multi-functionalized POSS cages. We highlight the self-assembled structures and physical properties of giant surfactants and chain-end- and side-chain-type hybrids derived from mono-functionalized POSS cages; main-chain-type hybrids derived from di-functionalized POSS cages; and star-shaped hybrids derived from multi-functionalized POSS cages; with various polymeric attachments, including polystyrene, poly(methyl methacrylate), phenolic, PVPh, and polypeptides.

## Introduction

Over the last four decades, self-assembled nanostructures obtained from organic surfactants and block copolymers (BCPs) have received much attention for nanopatterning, the formation of nanocomposites, and photonic crystals, and drug delivery because they can be prepared in simple and inexpensive methods.[1–10] These self-assembled nanostructures form from a combination of covalent bonding and repulsive noncovalent interactions, with the latter arising from the immiscibility of hydrophobic and hydrophilic segments. In the bulk state, these well-defined nanostructures can display alternative lamellae (LAM), double-gyroid (DG), hexagonally packed cylinder (HPC), face-centered cubic (FCC), and body-centered cubic (BCC) structures.[11–20] In some recent cases, Frank–Kasper (FK) phases (*e.g.*, A15 and σ phases) have also been observed between the HPC and BCC phases of the structures formed from surfactants and BCPs.[21–28] In solution,

*Department of Materials and Optoelectronic Science, Center for Functional Polymers and Supramolecular Materials, National Sun Yat-Sen University, Kaohsiung 80424, Taiwan. E-mail: kuosw@faculty.nsysu.edu.tw*

**Mohamed Gamal Mohamed**

*Mohamed Gamal Mohamed received his BSc in chemistry from Assiut University in 2004. Then, he received his MSc in applied chemistry at National Chiao Tung University under the supervision of Prof. Feng-Chih Chang in 2013. In 2016, he received his PhD from the National Sun Yat-Sen University in polymer chemistry under the supervision of Prof. Shiao-Wei Kuo. In 2017, He joined Prof. Tang's group at Hong Kong University of Science and Technology as a visitor researcher. He is currently pursuing his postdoctoral works also at National Sun Yat-Sen University during 2018 to present. His current research interests include polybenzoxazine, self-assembled nanostructure, polymer nanocomposites, and microporous conjugated polymers.*

**Shiao-Wei Kuo**

*Shiao-Wei Kuo received his BSc in chemical engineering from the National Chung Hsing University (1998) and PhD in applied chemistry from the National Chiao Tung University in Taiwan (2002). He continued his research work at Chiao Tung University as a postdoctoral researcher during 2002–2007 and also move to University of Akron as a postdoctoral researcher during 2005–2006. In 2007, be became as an assistant professor in the Department of Materials and Optoelectronic Science, National Sun Yat-Sen University, Taiwan. In 2022, he is the chair professor in the National Sun Yat-Sen University, Taiwan. His research interests include polymer interactions, self-assembly nanostructures, mesoporous materials, POSS nanocomposites, and polybenzoxazine, and covalent organic framework.*

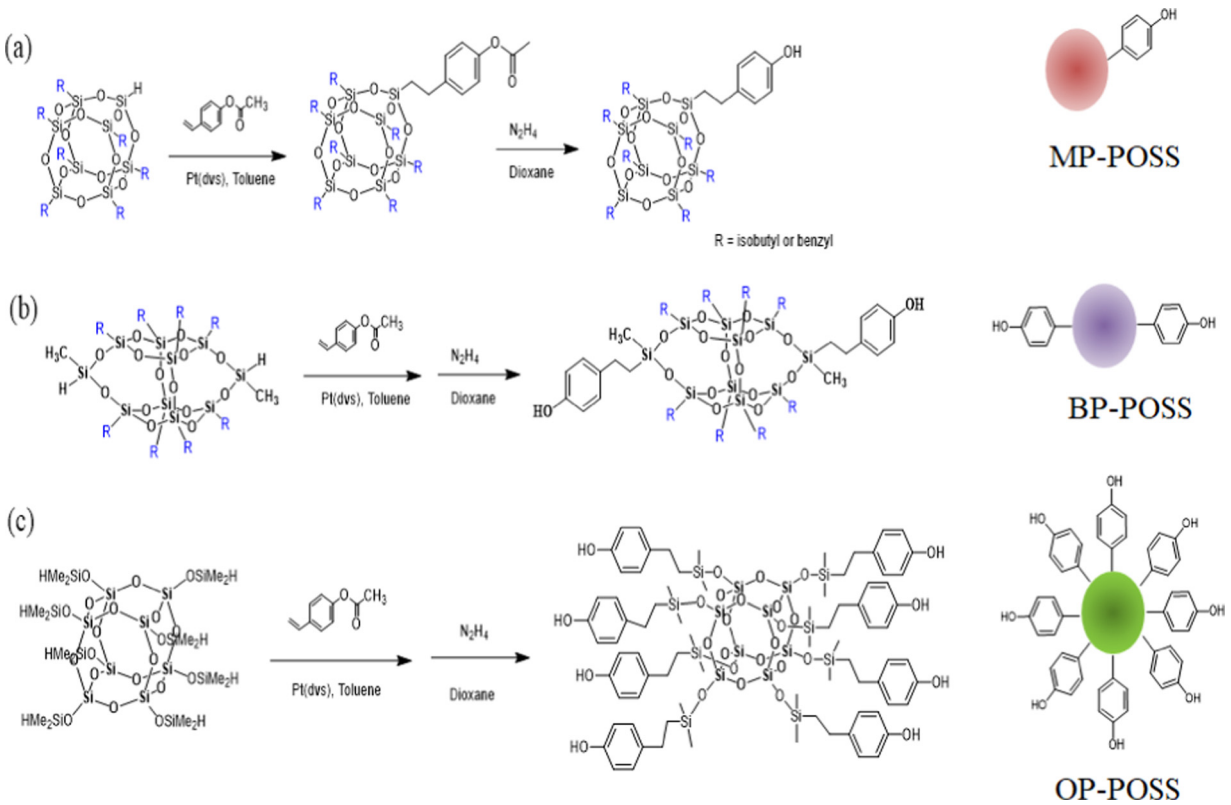


Fig. 1 Syntheses of (a) an MP-POSS (mono-functional POSS) cage from H-POSS, (b) a BP-POSS (di-functional POSS) cage from DDSQ, and (c) an OP-POSS (octa-functional POSS) cage from $Q_8M_8^H$, all through hydrosilylation and hydrolysis.[85]

these materials can also spontaneously form self-assembled nanostructures, including micellar, worm-like, and vesicle structures, with the type of nanostructure formed depending primarily on the volume fraction, interaction parameter ($\chi$), and degree of polymerization ($N$), but other factors (*e.g.*, common solvents, selective solvents, temperature, architecture, or terminal functional units) can also have strong influences.[29–32]

Incorporating or blending inorganic nanoparticles (NPs) at low concentrations into organic surfactants, polymeric materials, or BCPs can be a simple means of enhancing the thermal, mechanical, and optoelectronic properties of self-assembled organic materials.[33–42] Inorganic NPs blended into organic BCPs can resulting in the tuning of the self-assembled structures formed from the BCP/NP hybrids, their thermal and mechanical properties are generally not enhanced significantly.[43–51] As a result, organic–inorganic hybrid surfactants and BCPs connected by covalent bonds or electrostatic physical interaction have been attracting increased attention recently.[52–60] Various techniques including ring-opening polymerization (ROP), atom transfer radical polymerization (ATRP), reversible addition–fragmentation chain transfer (RAFT), controlled living radical polymerization (CLRP), and anionic polymerization which were used to incorporate POSS nanoparticles into polymer chain.[8] For example, polystyrene-*block*-polydimethylsiloxane (PS-*b*-PDMS) and polystyrene-*block*-poly(ferrocenyl dimethylsilane) (PS-*b*-PFS) organic–inorganic hybrid BCPs have been used in integrated circuit processing.[61–63] In addition, the smallest possible inorganic silica NP, polyhedral oligomeric silsesquioxane (POSS), has been used to prepare organic–inorganic surfactants and BCPs.[64–78] The presence of the POSS NPs within a surfactant or BCP can tune its self-assembly and its thermal and optoelectronic properties.[64–83] The properties of molecular nanoparticles based on gaint molecules depend on the primary structures. There are four types of macromolecular isomers (topo-isomers, sequence-isomers, regioisomers, and stereoisomers). Some factors are strongly influenced by the self-assembly of these four isomers such as the concerted interaction of each building block in a precise approach and the notable symmetry.[84] POSS NPs can be synthesized in mono-, di-, or multi-functionalized form (*e.g.*, with OH groups) to vary the degrees of macro-phase separation in resulting polymer/POSS hybrids, as displayed in Fig. 1.[85] This Review summarizes the self-assembly of organic–inorganic surfactant and BCP hybrids incorporating mono-, di-, and multi-functionalized POSS cages.

## Self-assembly of organic–inorganic polymer/POSS hybrids

POSS NPs presenting different numbers and types of functionalized organic units can be incorporated within polymeric materials through covalent bonding to enhance the thermal, mechanical, and oxidation properties of the polymers; as a result, studies of POSS-incorporated polymeric materials

 

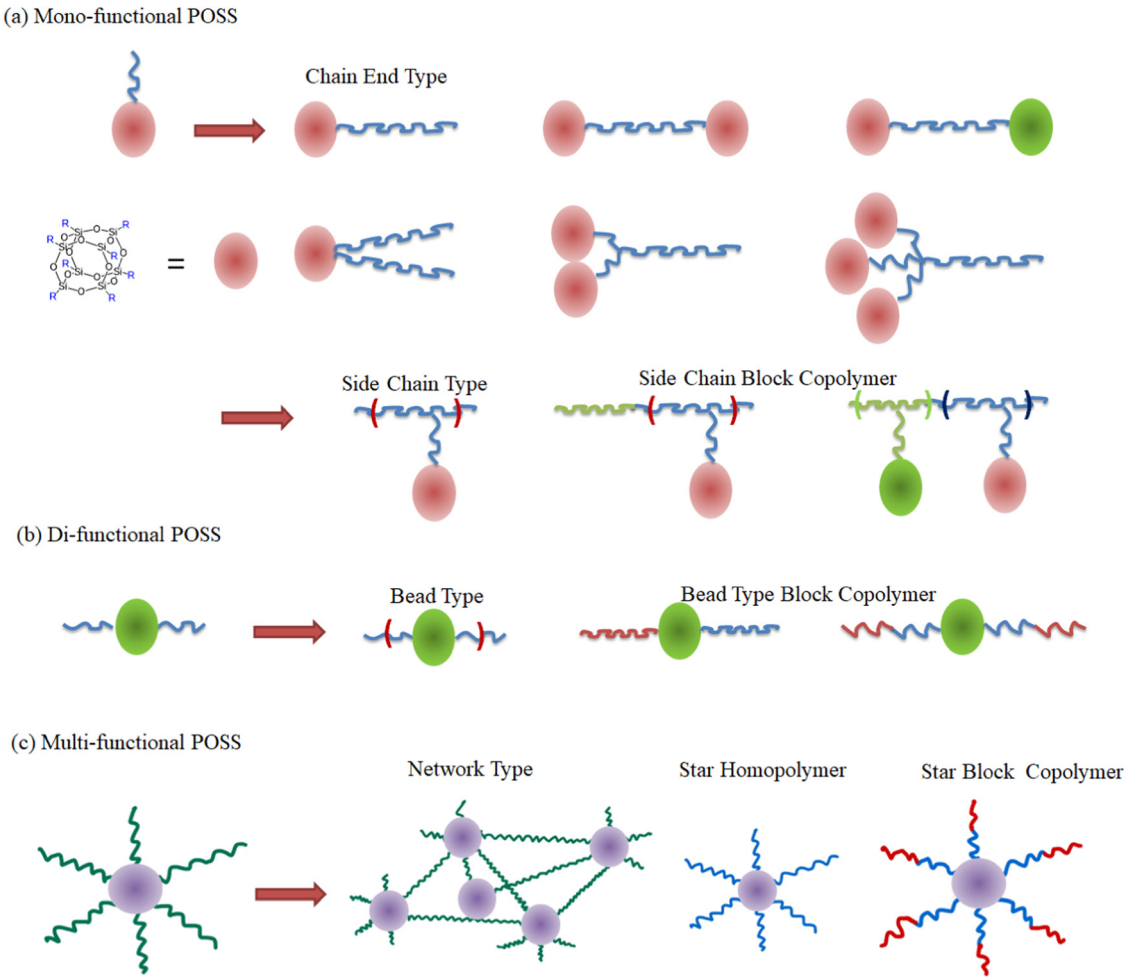


Fig. 2 Organic/inorganic POSS hybrids with various architectures formed from (a) mono-, (b) di-, and (c) multi-functionalized POSS cages.[93,94]

have increased significantly recently.[86–94] In this Review, we discuss the different functionalities and topologies presented by the POSS NPs, as displayed in Fig. 2.[93,94] In the following sections, we provide details of some representative examples of the self-assembly behavior of polymer/POSS hybrids.

### Self-assembly of chain-end-tethered mono-functionalized POSS NPs

Studies of the self-assembly of organic–inorganic polymer/POSS hybrids have focused mainly on the chain-end-tethered mono-functionalized POSS NPs.[95,96] In general, the syntheses of such polymer–POSS hybrids have been performed by using mono-functionalized POSS NPs as macro-initiators for living polymerizations [*e.g.*, anionic, cationic, ring opening polymerization (ROP), nitroxide-mediated polymerization (NMP), reversible addition-fragmentation chain transfer (RAFT), atom transfer radical polymerization (ATRP)] and click chemistry.[97–103] For example, we used a chain-end-tethered mono-functionalized chloride-POSS as a macroinitiator to prepare a poly(methyl methacrylate)–*block*–POSS (PMMA-*b*-POSS) hybrid through ATRP [Fig. 3(a)].[104] This PMMA-*b*-POSS hybrid behaved as a macromolecular or giant surfactant, where the PMMA segment was the long-chain hydrophobic tail and the POSS NP was the hydrophilic head, when blended with phenolic resin [Fig. 3(c)]. The strong intramolecular screening effect for this phenolic/PMMA-*b*-POSS hybrid [$\gamma$ = 0.65; Fig. 3(b)] indicated that the POSS NPs strongly inhibited intermolecular hydrogen bonding between the OH and C=O groups of the phenolic/PMMA pairs.[104]

We also prepared a chain-end-type poly($\gamma$-benzyl L-glutamate)–*block*–POSS (PBLG-*b*-POSS) hybrid from a mono-functionalized amino POSS derivative ($NH_2$-POSS) through *N*-carboxyanhydride (NCA) ROP [Fig. 4(a)] and examined its self-assembly behavior both in solution and in the solid state.[105] In the solid state, the presence of the POSS NP at the chain end enhanced the intramolecular hydrogen bonding of the PBLG block [Fig. 4(b)], thereby increasing the fraction of the $\alpha$-helix conformation; in solution, it prevented nanoribbon aggregation to form a clear gel. Fig. 4(c) and (d) present transmission electron microscopy (TEM) images of toluene solutions of the pure PBLG and the PBLG-*b*-POSS hybrid, respectively, at similar

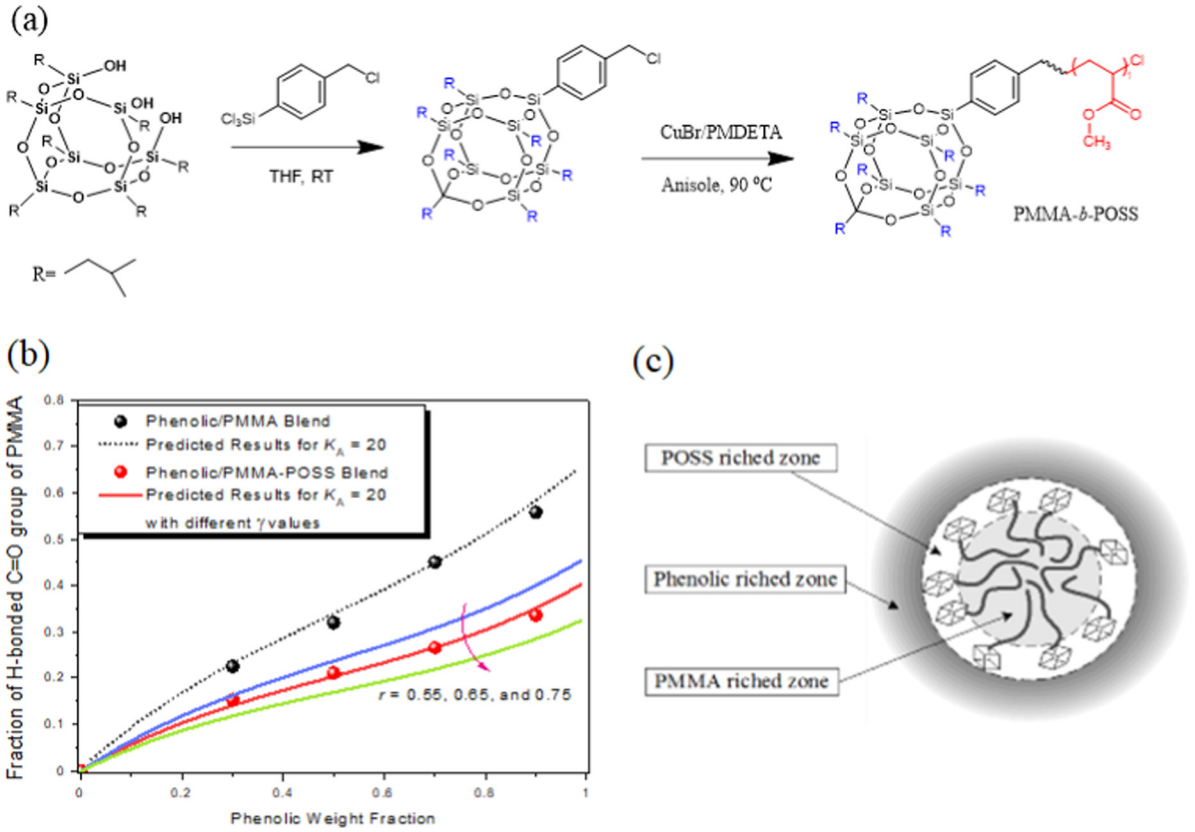


Fig. 3 Synthesis of PMMA-*b*-POSS through ATRP using POSS-Cl as a initiator. (b) Experimental and predicted fractions of hydrogen-bonded C═O groups and (c) screening effect of PMMA-*b*-POSS when blended with phenolic.[104] Reproduced from ref. 104 with permission from American Chemical Society.

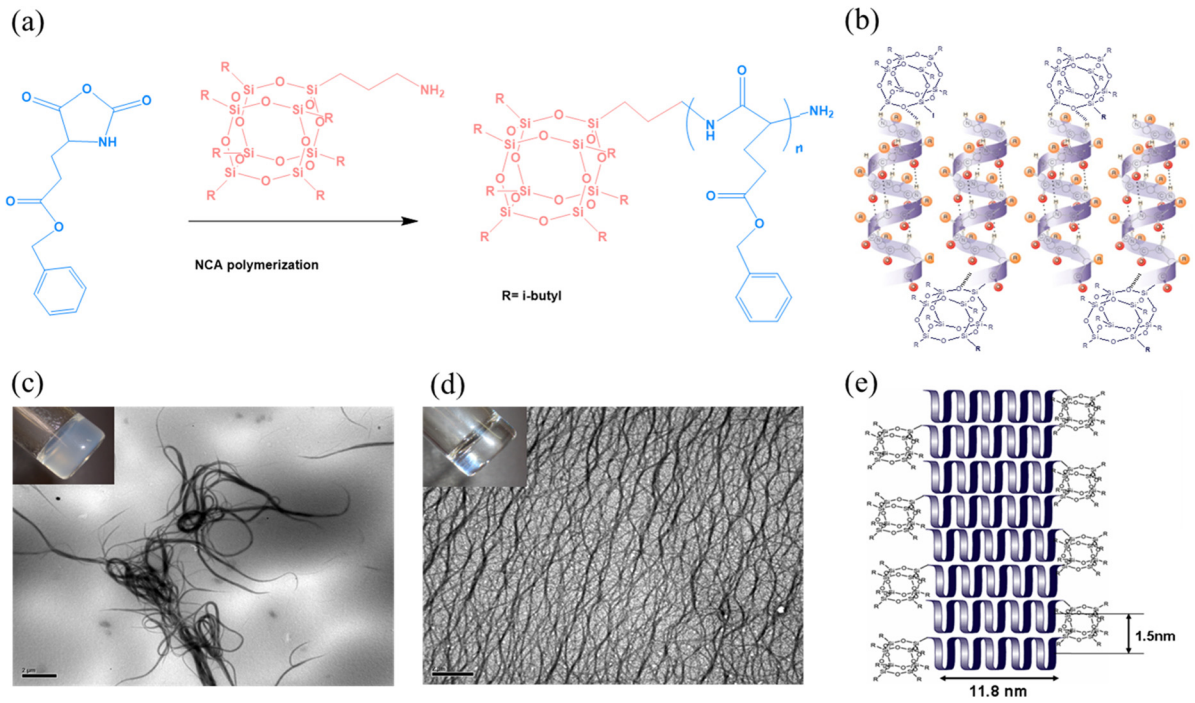


Fig. 4 (a) Synthesis of POSS-*b*-PBLG through NCA ROP using a mono-functionalized $NH_2$-POSS cage. (b) Possible intramolecular hydrogen bonds in a POSS-*b*-PBLG BCP. (c and d) TEM images of (c) pure PBLG and (d) POSS-*b*-PBLG in toluene. (e) Possible nanoribbon structure for POSS-*b*-PBLG in toluene.[105] Reproduced from ref. 105 with permission from American Chemical Society.

 

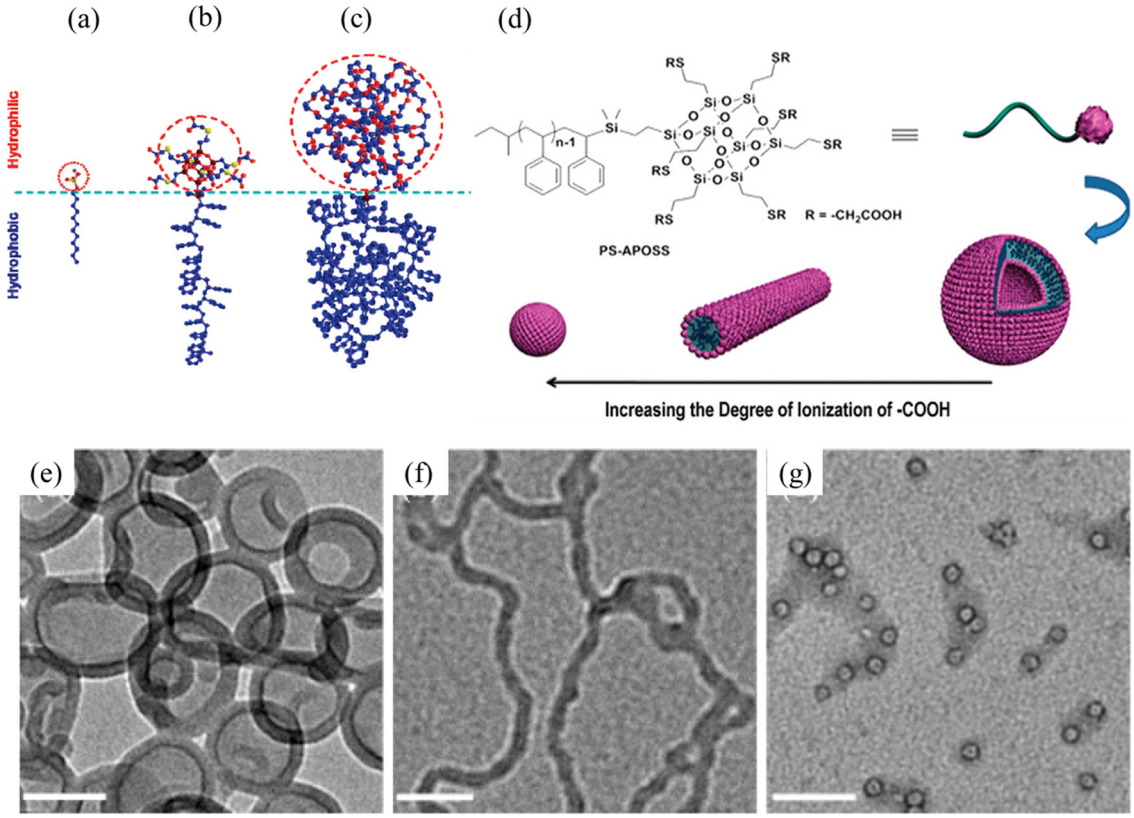


Fig. 5 (a–c) Chemical structures of (a) an surfactant, (b) a PS-APOSS giant surfactant, (c) an amphiphilic BCP. (d) Possible self-assembled structures formed from the PS-APOSS giant surfactant with various degrees of ionization. (e–g) TEM images of PS-APOSS in (e) 1,4 dioxane, (f) DMF, and (g) DMF/NaOH common solvents.[108] Reproduced from ref. 108 with permission from American Chemical Society.

degrees of polymerization (DPs). A turbid gel was formed from the pure PBLG, because strong π-stacking among its rigid rods stabilized these micro-fibers, forming irregular structures. In contrast, the PBLG-*b*-POSS hybrid formed a clear gel with ordered and oriented nanofibers(average width: *ca.* 10 nm). A possible anti-parallel arrangement of the PBLG-*b*-POSS hybrid [Fig. 4(e)] might have minimized the steric clashes of the POSS NPs, thereby inducing the self-assembly of nanofibers and the formation of a clear gel.[105] Similar chain-end-type PBLG-*b*-POSS hybrids have also been prepared by other groups; studies in the bulk and in solution have revealed that the chain length of the PBLG block strongly influences the secondary structure of the hybrids and their self-assembly.[52,105,106]

Couglin *et al.* used anionic living polymerization and condensation to prepare a well-defined hemi-telechelic PS-functionalized POSS, which introduced the self-assembly or aggregation behavior of POSS into the PS matrix.[107] Cheng *et al.* also prepared various PS chain-end-tethered mono-functionalized POSS NP hybrids, which formed many interesting self-assembled structures in the bulk and in solution; these giant POSS surfactants [Fig. 5(b)], featuring a long-chain PS hydrophobic tail and a POSS NP as a giant hydrophilic head, had properties similar to those of surfactants [Fig. 5(a)] and BCPs [Fig. 5(c)].[108] For example, they used anionic living polymerization, hydrosilylation, and click chemistry to prepare a hybrid featuring a well-defined PS hydrophobic tail and a carboxylic acid–functionalized POSS as the hydrophilic head [Fig. 5(d)]. In various selective solvents, this giant POSS surfactant formed micelles with various morphologies—from vesicles to wormlike cylinders, to spherical structures—upon tuning the degree of ionization of the carboxylic acid unit [Fig. 5(e)–(g)].[108] By varying the functional group on the POSS NP and varying the topology of the PS chain, the PS-*b*-POSS hybrids exhibited diverse molecular designs that underwent finely tuned self-assembly. By changing the volume fraction of the PS block, the PS-*b*-POSS hybrids formed various self-assembled structures, including LAM, DG, HEX, and BCC structures, in the bulk (Fig. 6), as characterized using small-angle X-ray scattering (SAXS) and TEM, with the phase diagram of the giant POSS surfactant being similar to that of organic diblock copolymers.[109] Yang and his group successfully prepared giant amphiphiles consisting of polyhedral POSS derivatives and PEO and these materials could be formed a fractal pattern in the LB monolayer.[110]

More interestingly, Cheng *et al.* observed that POSS NPs presenting various organic functional groups or polymer chains formed various FK phases, including σ, A15, and Z phases.[111] For example, three hydrophobic and one hydrophilic POSS

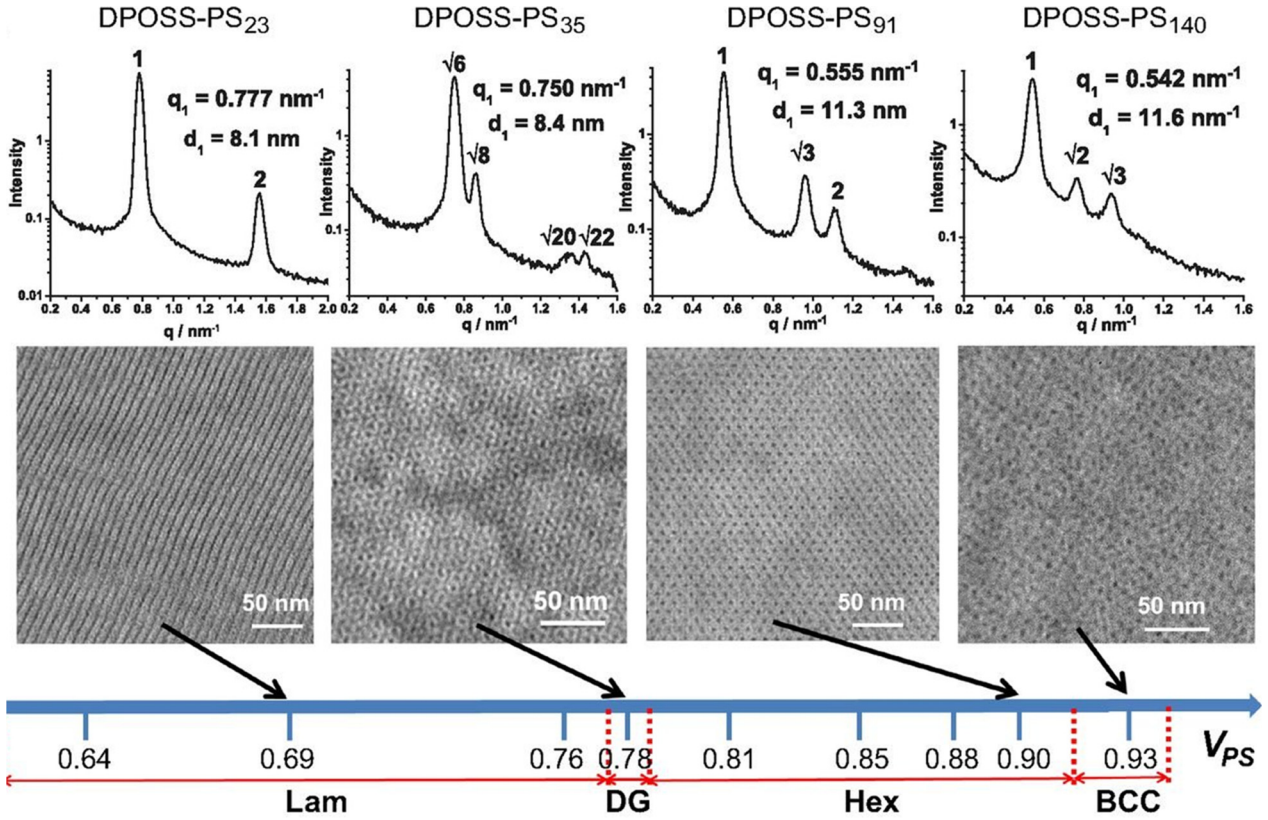


Fig. 6 SAXS patterns and TEM images of various DPOSS-PS giant surfactants (DPOSS-$PS_{23}$, DPOSS-$PS_{35}$, DPOSS-$PS_{91}$, and DPOSS-$PS_{140}$), where the POSS domains appear darker than the PS domains; corresponding phase diagram of these DPOSS-PS giant surfactants.[109] Reproduced from ref. 109 with permission from National Academy of Sciences USA.

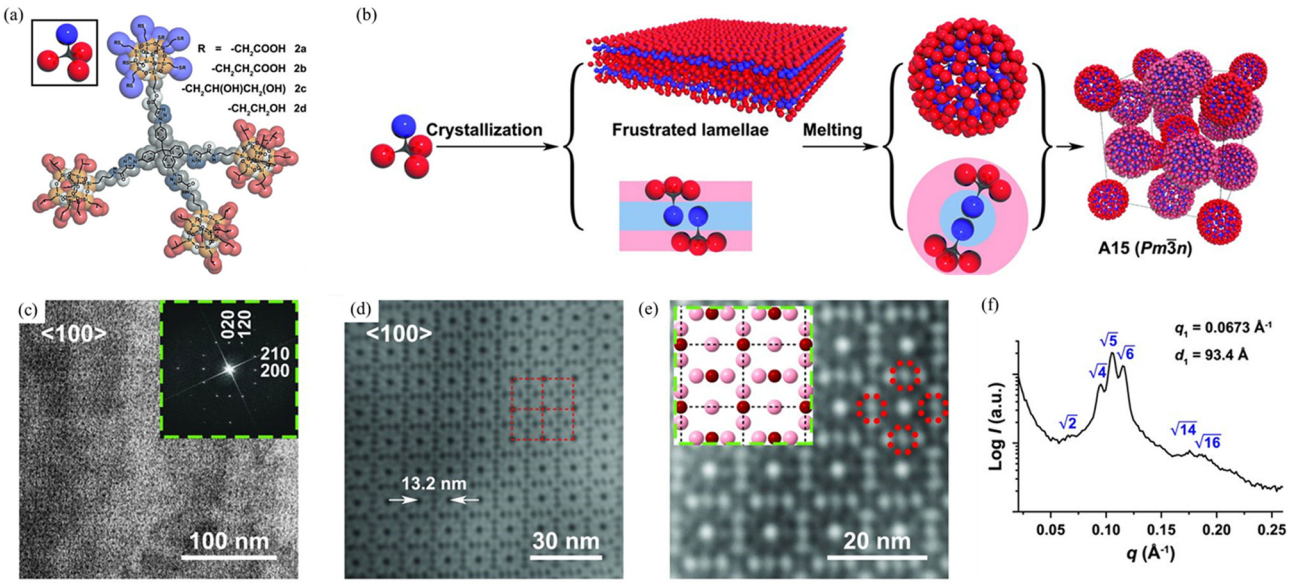


Fig. 7 (a) Chemical structure of giant tetrahedron based on POSS cages; red spheres are hydrophobic POSS cages; blue spheres are hydrophilic POSS cages. (b) Mechanism of self-assembly of the giant tetrahedron and molecular packing of the A15 phase (c) TEM image of the A15 phase. (d) Fourier filtering of the image in (c) of the $4^4$ tiling along the [100] direction. (e) Inverse coloring of the image in (d), where the spheres are hydrophilic POSS cages of various sizes. (f) SAXS pattern of the giant tetrahedron based on POSS cages.[111] Reproduced from ref. 111 with permission from Science.

 

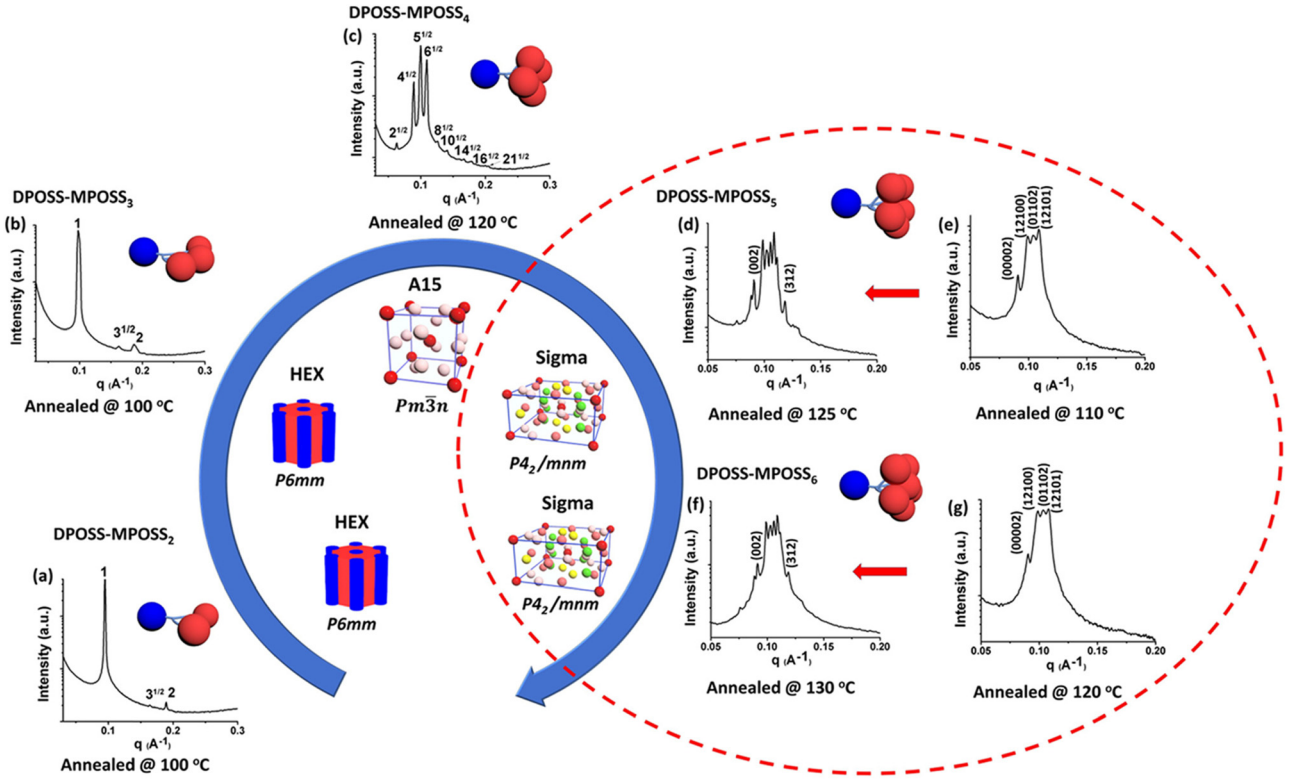


Fig. 8 SAXS patterns and the corresponding phase diagram of various $AB_n$ dendron-like giant surfactants: (a and b) HPC structures of (a) DPOSS-$MPOSS_2$ and (b) DPOSS-$MPOSS_3$; (c) A15 phase of DPOSS-$MPOSS_4$; (d) DQC structure and (e) σ phase of DPOSS-$MPOSS_5$ after annealing at 110 and 125 °C, respectively; (f) DQC structure and (g) σ phase of DPOSS-$MPOSS_6$ after annealing at 120 and 130 °C, respectively.[113] Reproduced from ref. 113 with permission from American Chemical Society.

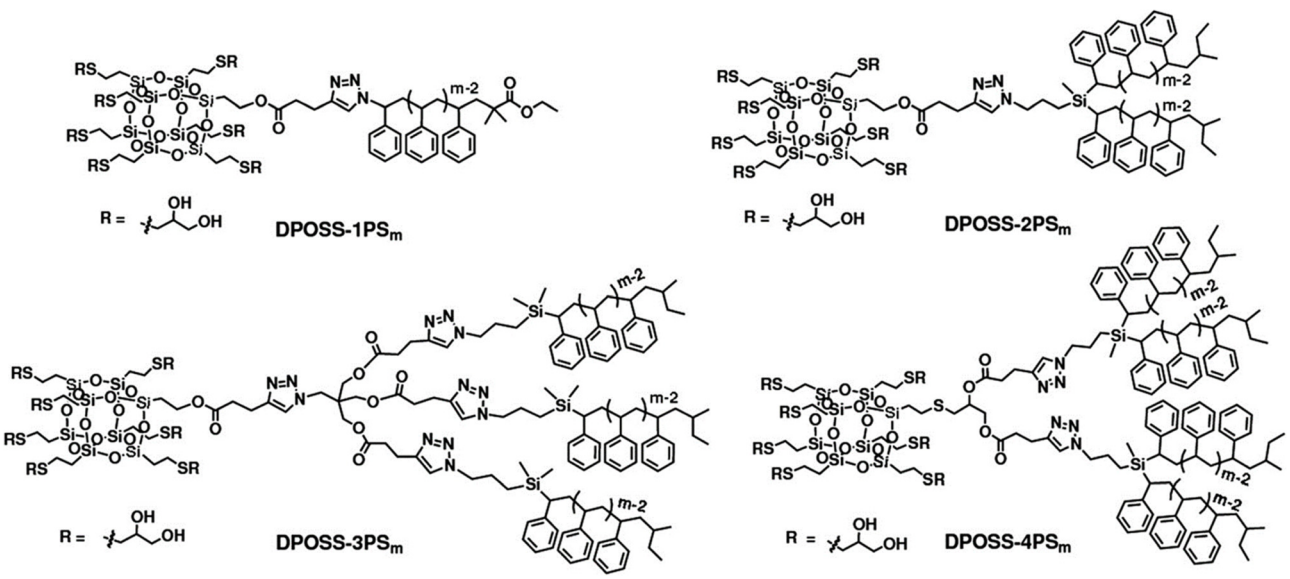


Fig. 9 Chemical structures of giant surfactants of DPOSS-$nPS_m$ where $n$ is the number of PS tails and $m$ is the degree of polymerization of each PS tail.[114] Reproduced from ref. 114 with permission from National Academy of Sciences USA.

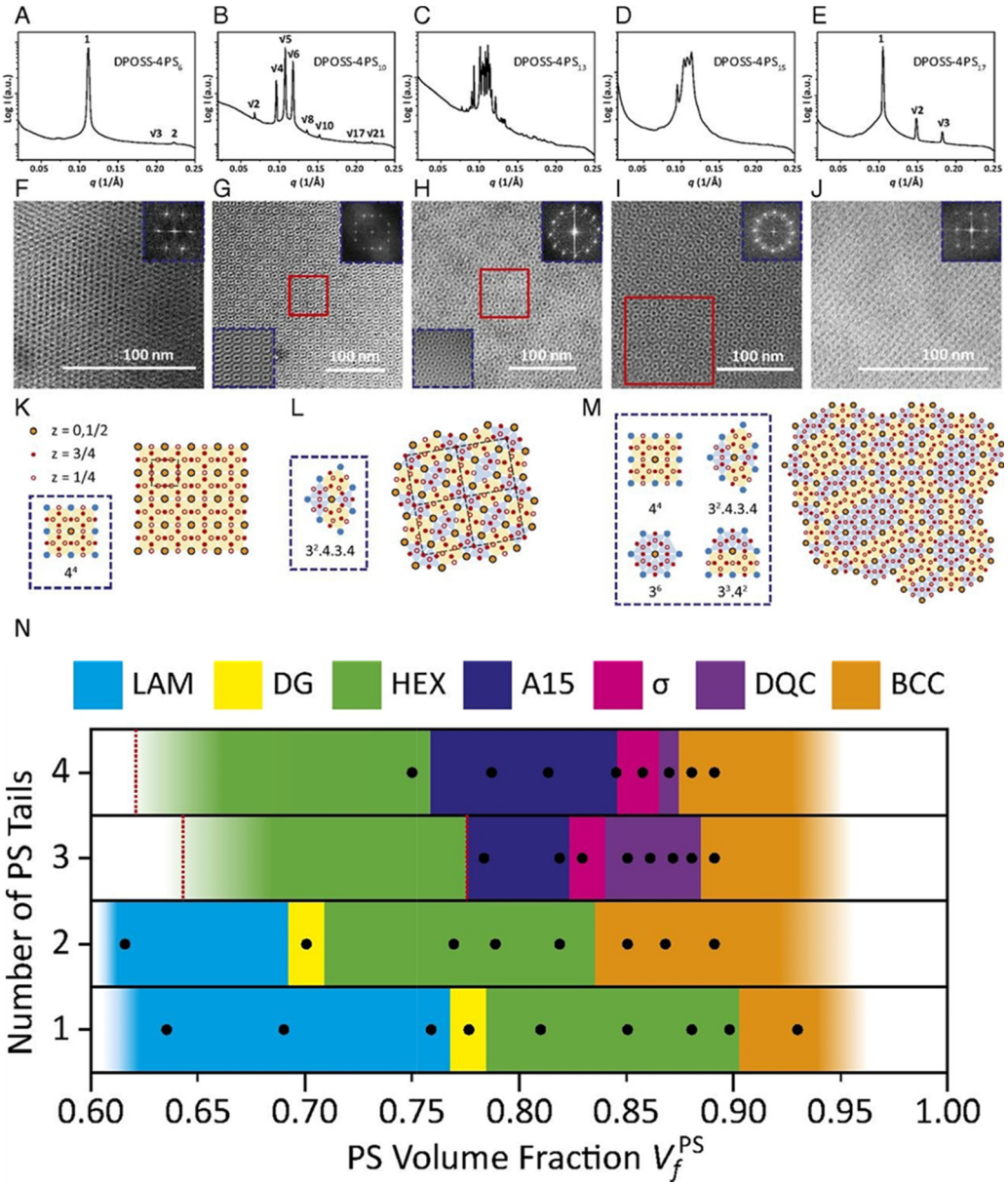


Fig. 10 SAXD, TEM, FFT patterns, and Fourier filtering analyses of various DPOSS-4PS$_m$ species. (A and F) HPC phase of DPOSS-4PS6; (B and G) A15 phase of DPOSS-PS10; (C and H) σ phase of DPOSS-4PS13; (D and I) DQC phase of DPOSS-4PS15; and (E and J) BCC phase of DPOSS-4PS17. 2D tilting patterns from (G–I) by the red-line box: (K) A15 phase, (L) σ phase, and (M) DQC phase. (N) Experimental phase diagram of the DPOSS-*n*PS$_m$ giant surfactant.[114] Reproduced from ref. 114 with permission from National Academy of Sciences USA.

units [Fig. 7(a)] bonded in the form of an giant amphiphilic tetrahedron self-assembled through molecular packing [Fig. 7(b)] and also formed the A15 phase [Fig. 7(c)–(e)].[111] FK phases are more commonly found in metal alloys having highly ordered and local complex lattice structures; nevertheless, self-assembled structures formed from soft matter (*e.g.*, liquid crystals, surfactants, BCPs, and giant amphiphiles) can also for FK A15, C14, C15, σ, H, and Z phases.[111] Fig. 7(c)–(e) reveal that the typical $4^4$ tiling number of the A15 phase was observed for the giant amphiphilic tetrahedron along the [001] zone; this phase was confirmed using SAXS [Fig. 7(f)], with a peak ratio of $\sqrt{2}:\sqrt{4}:\sqrt{5}:\sqrt{6}$ that is characteristic of the A15 phase.[111] Cheng *et al.* also synthesized giant amphiphilic molecules with six POSS cages grafted onto a triphenylene core; it self-assembled into the Z phase, with a typical $3^6$ tiling number.[112] A study of the non-crystalline dendron giant surfactant DPOSS-MPOSS$_n$, containing hydrophobic DPOSS and hydrophilic MPOSS cages (where $n$ is the number of hydrophilic MPOSS cages), revealed that increasing the value of $n$ caused the phases of the series of DPOSS-MPOSS$_n$ derivatives to change from HPC, to the FK A15 phase, and then to the σ phase (Fig. 8).[113] Furthermore, hydrophilic POSS units and various topologies

 

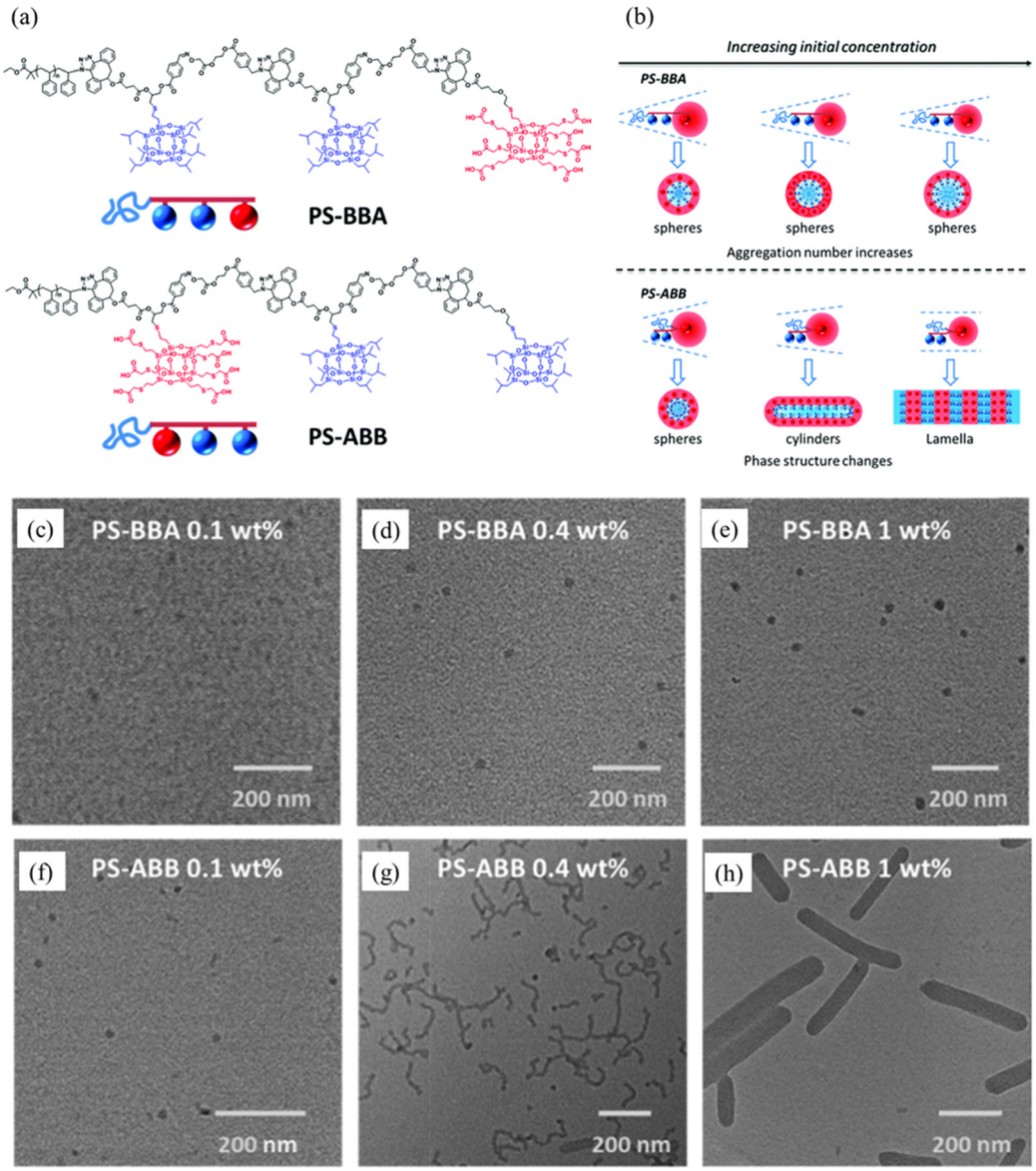


Fig. 11 (a) Chemical structures and (b) self-assembly procedures for PS-ABB and PS-BBA. (c–f) TEM analyses of the self-assembled structures of (c–e) PS-BBA and (f–h) PS-ABB at initial concentrations of (c and f) 0.1, (d and g) 0.4, and (e and h) 1 wt%.[115] Reproduced from ref. 115 with permission from the Royal Society of Chemistry.

of long-chain PS (as hydrophobic tails) have been used to prepare DPOSS-*N*PS$_m$ giant surfactants, where $m$ is the molecular weight and $N$ is the number of PS tails (Fig. 9).[114] The self-assembled structures formed from these giant POSS surfactants were strongly dependent on the molecular geometry. Quasicrystal and FK phases were stabilized in several regions, with typical A15, σ, DDQC, and BCC structures observed [Fig. 10(A)–(M)]; Fig. 10(N) summarizes the phase diagram of these DPOSS-*N*PS$_m$ derivatives.[114]

The molecular conformational packing of two kinds of macromolecular isomeric surfactants [PS-BBA and PS-ABB; Fig. 11(a)], based on PS and POSS cages, was found to depend on the arrangement of the POSS NP sequences.[115] Furthermore, these two macromolecules formed different self-assembled structures in DMF/water solution: a sphere morphology for PS-BBA [Fig. 11(b)–(e)] and sphere, cylinder, and lamella structures for PS-ABB [Fig. 11(f)–(i)]. Similarly, Liu *et al.* precisely constructed side-chain-functionalized giant compounds of various compositions and lengths through a deprotection and addition cycle approach. Using a solvent evaporation method, sandwiched two-dimensional (2D) nanosheet structures formed through self-assembly of these giant molecules, with the thickness of the 2D nanosheets being controlled by changing the BPOSS to APOSS ratios.[116] Cheng *et al.* prepared two different tri-armed POSS derivatives, tri-PS-APOSS and tri-APOSS, containing carboxylic acid groups, with

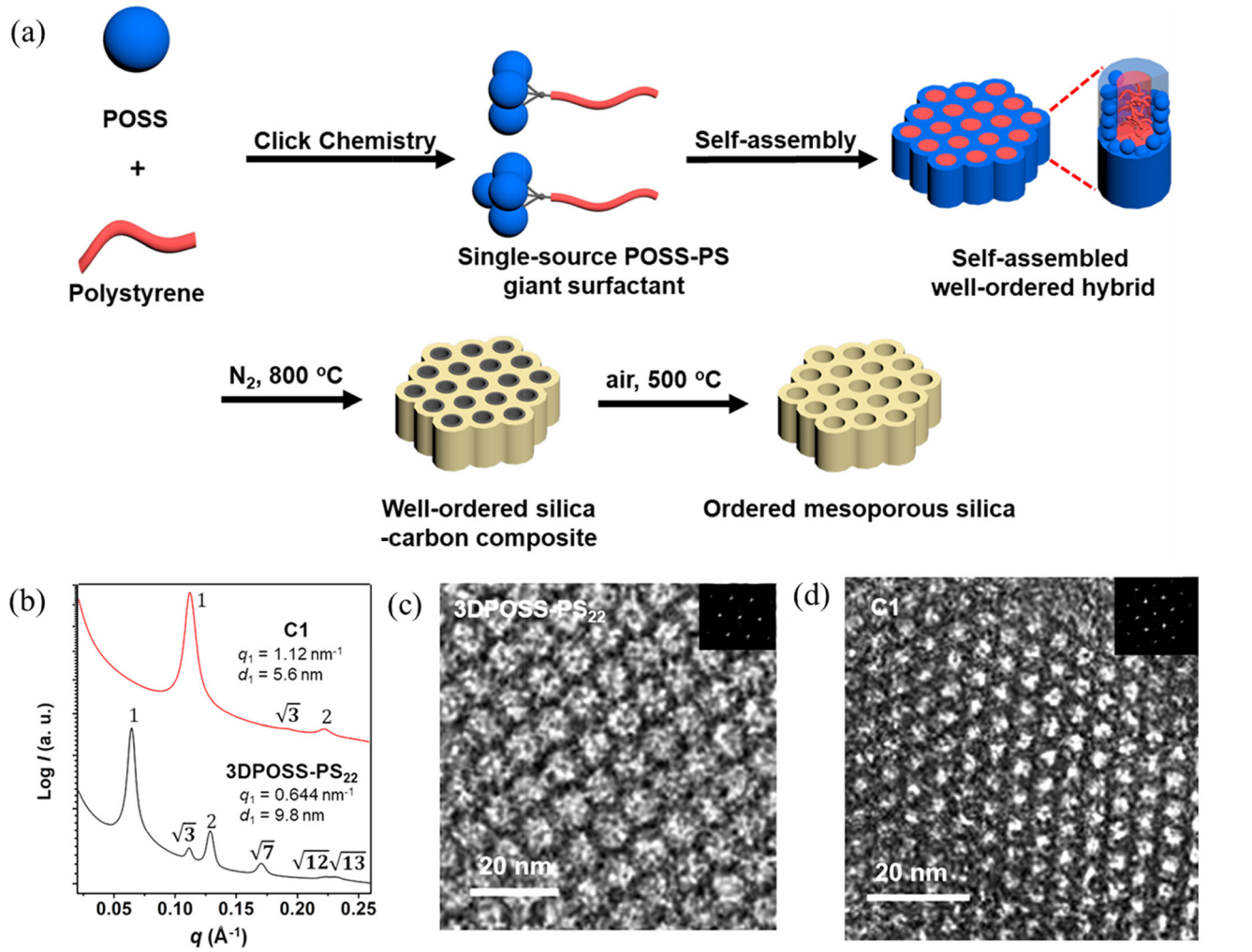


Fig. 12 (a) Synthesis of highly ordered mesoporous silica from a giant POSS surfactant. (b) SAXS patterns of self-assembled 3DPOSS-$PS_{22}$ and the corresponding mesoporous silica and (c and d) corresponding TEM images recorded (c) before and (d) after pyrolysis.[119] Reproduced from ref. 119 with permission from American Chemical Society.

the presence and absence of PS linkers, respectively, and examined their morphologies in solution. TEM images revealed that bilayer vesicles formed when the PS linker was present, whereas a hybrid morphology (single-layered and blackberry structures) formed in the absence of PS.[117] Wang *et al.* used isocyanate–amine reactions to prepare a giant POSS–ATA material containing POSS and doped tetraaniline (ATA) units. This micro-flower POSS–ATA structure exhibited high capacitance, high redox activity, corrosion inhibition, and excellent solubility in organic solvents.[118] Interestingly, Cheng *et al.* constructed highly ordered hexagonal mesoporous silicas of high surface area (581 $m^2\ g^{-1}$) and uniform pore size (3.3 nm) from a series of DPOSS-PS giant surfactants, after thermal treatment at 800 °C under $N_2$ and then at 500 °C in air [Fig. 12(a)].[119] Fig. 12(b)–(d) display SAXS patterns and TEM images of these samples. The 3DPOSS-PS material provided a peak ratio of $1:\sqrt{3}:\sqrt{4}:\sqrt{7}:\sqrt{12}:\sqrt{13}$, characteristic of the long-range order of an HPC structure [Fig. 12(b)], the presence of which was confirmed using TEM [Fig. 12(c)]. The SAXS pattern of the pyrolyzed sample obtained from 3DPOSS-PS also displayed a high-order peak ratio of $1:\sqrt{3}:\sqrt{4}$, indicating the preservation of the HPC structure in the mesoporous silica, again confirmed using TEM [Fig. 12(d)]. The primary *d*-spacing decreased from 9.8 to 5.6 nm after pyrolysis, implying that volume shrinkage occurred upon removal of the organic components.[119]

Liu *et al.* used a deprotection–addition approach to prepare two groups of single-chain giant molecules (SCGMs) and then studied their crystallization behavior.[120] The SCGMs containing non-ionic, cationic, or anionic hydrophilic segments formed 2D crystal structures, with the thicknesses and morphologies being unaffected by the sequence of the giant monomers.[120] Kim *et al.* prepared giant amphiphiles of poly(ethylene glycol)-PS–*block*–POSS (PEG-POSS-*b*-PS) of various molecular weights and studied the self-assembly in dioxane and acetone as common solvents. Steric clashes between the hydrophilic POSS

 

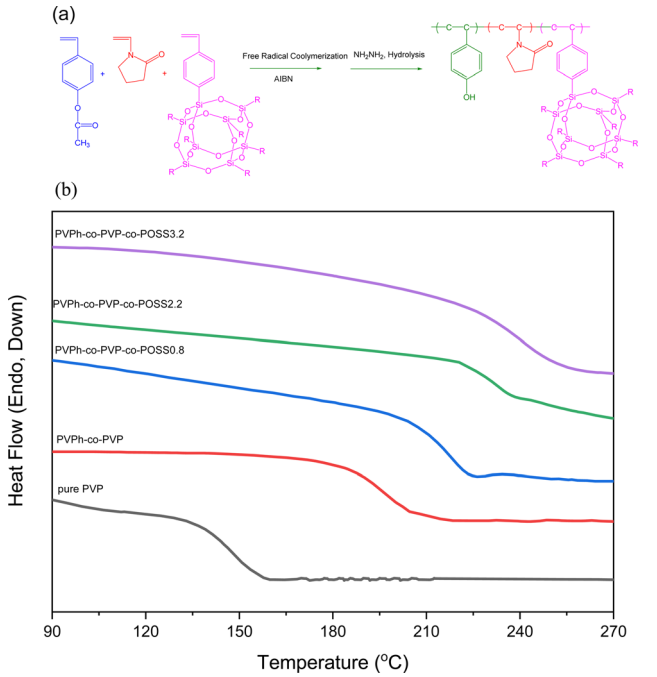


Fig. 13 (a) Chemical structures and synthesis of PVPh-*co*-PVP-*co*-POSS hybrids obtained through random copolymerization and hydrolysis. (b) DSC analyses of pure PVP, pure PVPh-*co*-PVP random copolymer, and PVPh-*co*-PVP-*co*-POSS hybrids with various POSS contents.[123,124] Reproduced from ref. 123 with permission from Elsevier. Reproduced from ref. 124 with permission from American Chemical Society.

blocks led to the PEG-POSS-*b*-PS copolymers self-assembling into polymer cubosomes, with a cubic phase clearly evident in the cubosomes.[121]

### Self-assembled behavior of side-chain-tethered mono-functionalized POSS NPs

The presence of side-chain-tethered mono-functionalized POSS cages can typically improve the thermal, mechanical, and optoelectronic properties of a polymeric matrix.[122] For example, we used free radical copolymerization of a mono-functionalized styrene-POSS cage to synthesize poly(hydroxystyrene-*co*-vinylpyrrolidone-*co*-isobutylstyryl polyhedral oligosilsesquioxanes) PVPh-*co*-PVP-POSS random copolymers with various compositions of styrene-POSS [Fig. 13(a)].[123,124] Because of strong hydrogen bonding between the OH groups of PVPh and the C=O groups of PVP and the Si–O–Si units of POSS, the glass transition temperature ($T_g$) of the PVPh-*co*-PVP-*co*-PS copolymer containing 3.2 mol% of styrene-POSS (245 °C) was much higher than those of the pure PVP and pure PVPh (150 °C) [Fig. 13(b)]. In addition, POSS cages have been grafted onto the side chains of PMMA through anionic living polymerization to form a PMA–POSS homopolymer [Fig. 14(a)].[125] A strong screening effect ($\gamma$ = 1) was observed for this PMA–POSS homopolymer upon blending PVPh, phenolic, and bisphenol A, indicating that the C=O groups of PMA–POSS could not interact with the OH group of the added polymers [Fig. 14(c)]; the phenolic/PMMA blend could, however, form

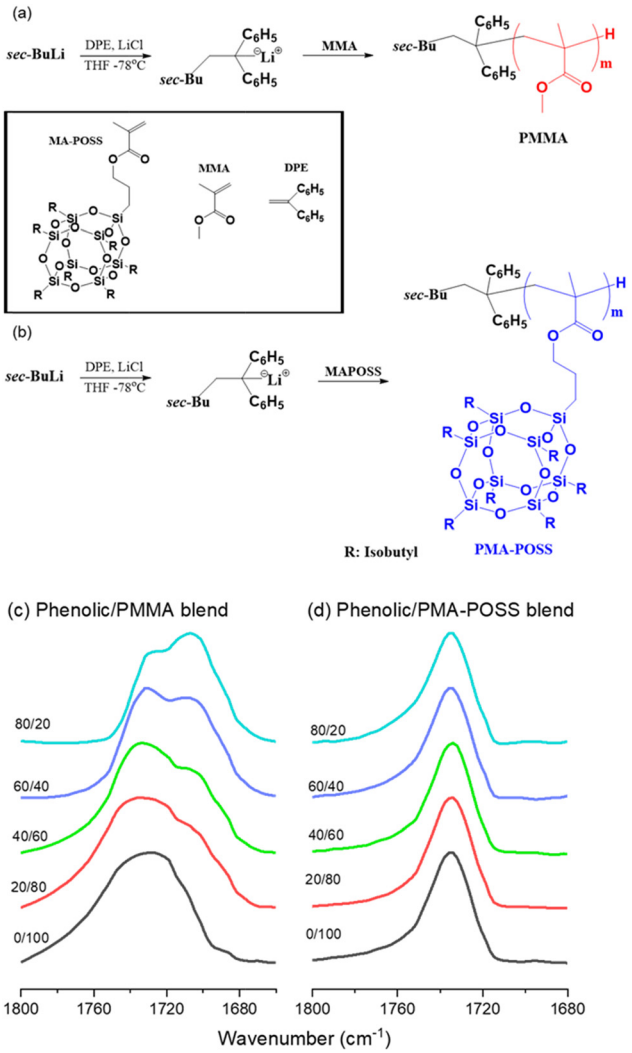


Fig. 14 (a and b) Anionic living polymerizations for the synthesis (a) pure PMMA and (b) pure PMAPOSS homopolymers. (c and d) FTIR spectral analyses of (c) phenolic/PMMA and (d) phenolic/PMAPOSS blends.[125] Reproduced from ref. 125 with permission from MDPI.

intermolecular hydrogen bonds upon increasing the phenolic concentration [Fig. 14(b)].

Based on this phenomenon, we prepared polypeptides featuring POSS cages grafted on their side chains.[128] We used a combination of NCA ROP (with *r*-propynyl-L-glutamate as the monomer) and click chemistry (with a mono-azido-functionalized $N_3$-POSS cage) to synthesize these PPLG-*g*-POSS homopolymers [Fig. 15(a)].[126] All of these PPLG-*g*-POSS polypeptides exhibited the α-helical secondary structure, even at very low DP, unlike the pure PPLG homopolymer. Because the POSS cages on the side chains induced a very strong screening effect and hindered intermolecular hydrogen bonding among the polypeptides, intramolecular hydrogen bonding of the polypeptides was facilitated, thereby encouraging the formation of α-helical secondary structures. We have also found that positioning other bulky units (*e.g.*, pyrene, cyclodextrin) or hydrogen bonding groups on the side chains of PPLG can

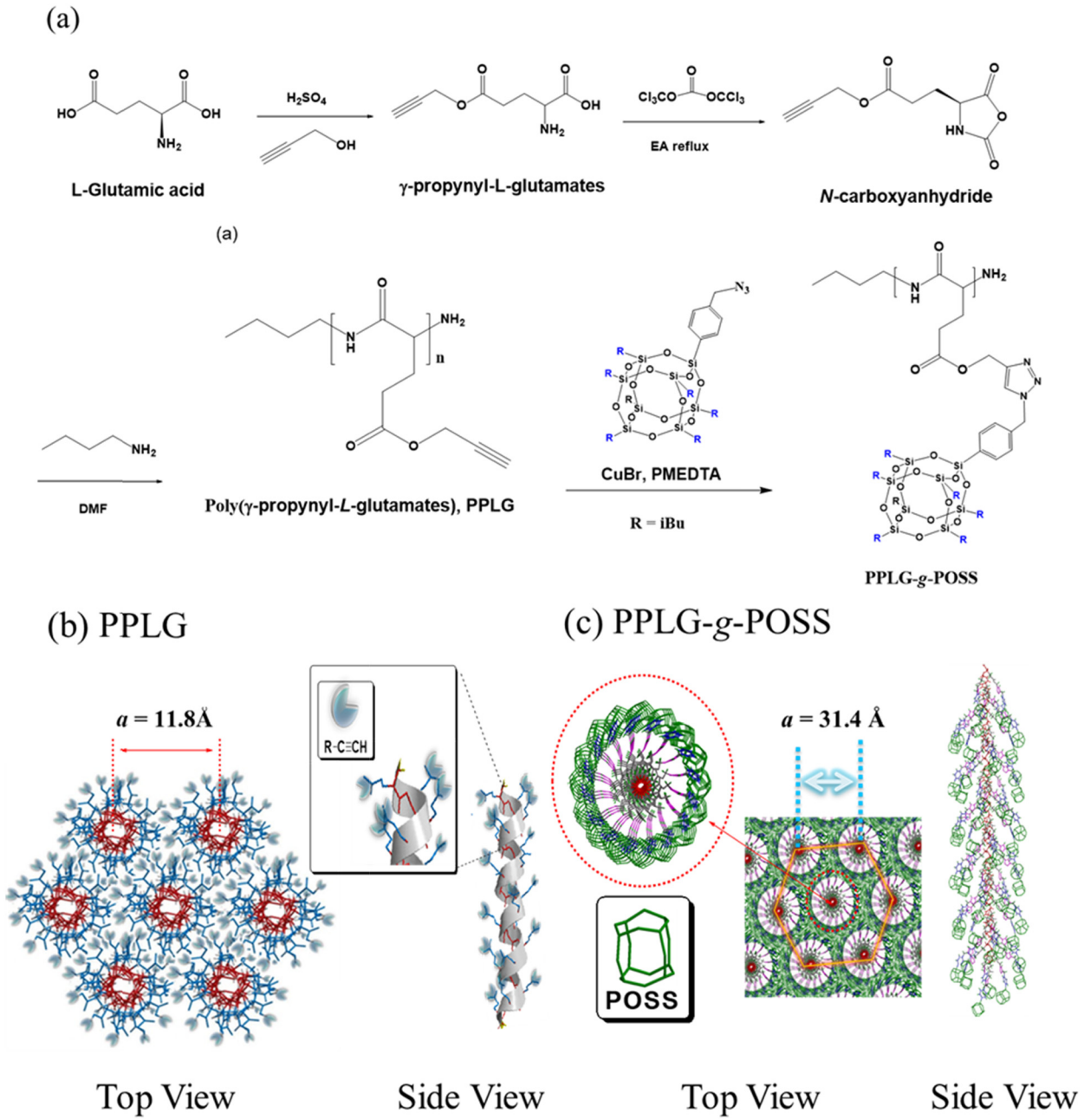


Fig. 15 (a) Synthesis of PPLG-*g*-POSS from PPLG and mono-functionalized $N_3$-POSS through click reaction. (b and c) Self-assembled structures of (b) pure PPLG and (c) PPLG-*g*-POSS.[126] Reproduced from ref. 126 with permission from the Royal Society of Chemistry.

enhance the formation of α-helical conformations.[126] Furthermore, wide-angle X-ray diffraction (WAXD) of PPLG revealed that the strong first peak appeared at $q$ = 0.58 $nm^{-1}$, close to that for the α-helical conformation, with a $d$-spacing of 1.18 nm, suggesting an HPC structure [Fig. 15(b)]; for PPLG-*g*-POSS, the pattern featured a strong diffraction angle ($q$ = 0.2 $nm^{-1}$) and a weak diffraction angle (at $q$ = 0.35 $nm^{-1}$) with a relative position ratio of $1:3^{1/2}$, again corresponding to a 2D HPC structure with a $d$-spacing of 3.14 nm [Fig. 15(c)].[126]

Several other organic–inorganic BCPs based on POSS cages have been studied during the last decade.[127–131] Pyun and Matyjaszewski prepared PMAPOSS from *n*-butyl acrylate monomers to form methacryloyl POSS BCPs.[132] Hayakawa *et al.* used sequential anionic living polymerization to synthesize PMMA-*b*-PMAPOSS and PS-*b*-PMAPOSS [Fig. 16(a) and (b)] and observed (SAXS, TEM) various self-assembled nanostructures (including LAM, HPC, and spherical structures) [Fig. 16(c)–(o)] for these PMAPOSS based on BCPs.[133] We extended these BCPs with various volume fractions of each segment and then blended

 

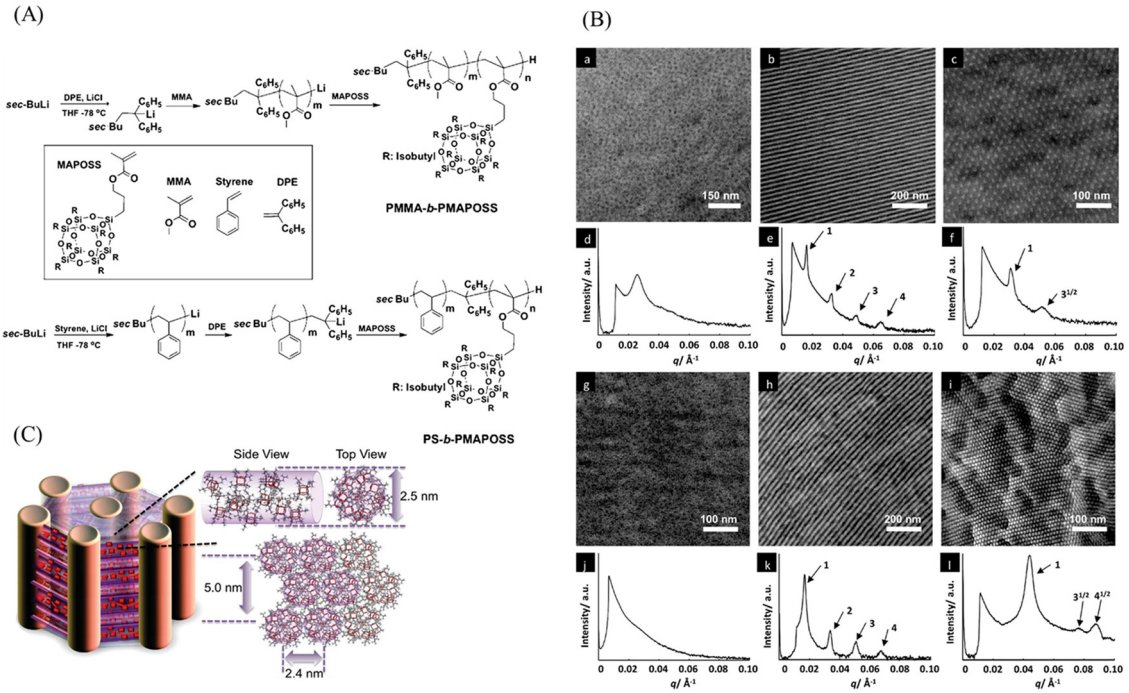


Fig. 16 (A) Synthesis of PMMA-*b*-PMAPOSS and PS-*b*-PMAPOSS diblock copolymers through anionic living polymerization. (B) TEM and SAXS analyses of (a and d) $PMMA_{450}$-*b*-$PMAPOSS_7$, (b and e) $PMMA_{262}$-*b*-$PMAPOSS_{23}$, (c and f) $PMMA_{52}$-*b*-$PMAPOSS_{18}$, (g and j) $PS_{587}$-*b*-$PMAPOSS_4$, (h and k) $PS_{266}$-*b*-$PMAPOSS_{20}$, and (i and l) $PS_{52}$-*b*-$PMAPOSS_9$. (C) Self-assembled structures of PMMA-*b*-PMAPOSS copolymers and HPC PMMA in a PMAPOSS matrix, where the PMAPOSS segment has a helix-like structure.[133] Reproduced from ref. 133 with permission from American Chemical Society.

them with phenolic resin (Fig. 17). Because the OH groups of phenolic interact only with the C=O groups of PMMA, and not with the C=O groups of PMAPOSS, we observed (TEM, SAXS) an order-order self-assembled nanostructure transition upon blending these BCPs with phenolic [Fig. 17(a)–(h)]. Upon increasing the concentration of phenolic, TEM imaging revealed that the PMMA-*b*-PMAPOSS BCP transitioned from an HPC structure to an LAM structure and finally to an onion-like structure, suggesting that this blend system exhibited wet-brush behavior, due to ready variation of the PMAPOSS volume fraction when blending with phenolic. Fig. 17(i) summarizes the phase diagram of the phenolic/PMMA-*b*-PMAPOSS blends.[134] Similarly, PS-*b*-(PPLG-*g*-POSS) bock copolymers have been prepared using a combination of ATRP, NCA-ROP, and click chemistry [Fig. 18(a)].[135] Fourier transform infrared (FTIR) spectra revealed that the α-helical conformation was enhanced by the presence of both the POSS cage and the PS segment, as measured in the solid state at various temperatures. SAXS [Fig. 18(b) and (c)] and TEM [Fig. 18(d) and (e)] analyses indicated that the PS-*b*-PPLG and PS-*b*-(PPLG-*g*-POSS) copolymers possessed HPC structures, arising from the α-helical conformation of the polypeptide and the self-assembled structure of the copolymer, with each structure perpendicularly oriented [Fig. 18(f) and (g)].

Zheng *et al.* used sequential RAFT polymerization to prepare a series of POSS-*b*-PAA-*b*-POSS copolymers. In aqueous solution, TEM images revealed that these triblock copolymers formed spherical nanoobjects.[136] In the bulk state, these triblock copolymers formed microphase-separated structures, with the POSS blocks residing in microdomains in the PAA matrix, according to SAXS and TEM analyses.[136] Interestingly, Zhang *et al.* used RAFT polymerization and doping to synthesize various POSS-functionalized liquid-crystalline PHEMA-POSS-*b*-P6CBMA BCPs, with the POSS unit and the mesogenic cyanobiphenyl block stabilizing blue-phase liquid crystals (LCs). The doped LC BCP materials had a lower hysteresis and driving voltage, excellent thermal stability, and a higher value of Kerr constant K.[137] The Dai group used ATRP to prepare stimuli-responsive PEG-*b*-P(MAPOSS-*co*-DPA) polymeric systems. This series of POSS-based amphiphilic copolymers formed spherical micelles with a core–shell structure, with average diameters in the range 158–223 nm, based on TEM imaging and dynamic light scattering (DLS) (Fig. 19).[138] Lee *et al.* prepared three different norbornene-substituted POSS monomers for the synthesis of rod-like POSS-containing polynorbornenes, through facile ring-opening metathesis polymerization (ROMP). They then prepared rod-like POSS-bottlebrush BCPs (BBCPs) through sequential ROMP of POSS norbornenes Interestingly, the thin films of the POSS-BBCPs self-assembled into ordered nanostructures with various morphologies and periodicities of greater than 100 nm.[139] Wang *et al.* used ROMP with Grubbs catalysts to prepare multi-cluster-wrapped polymers and their block bottlebrush copolymers with highly controlled compositions and chain

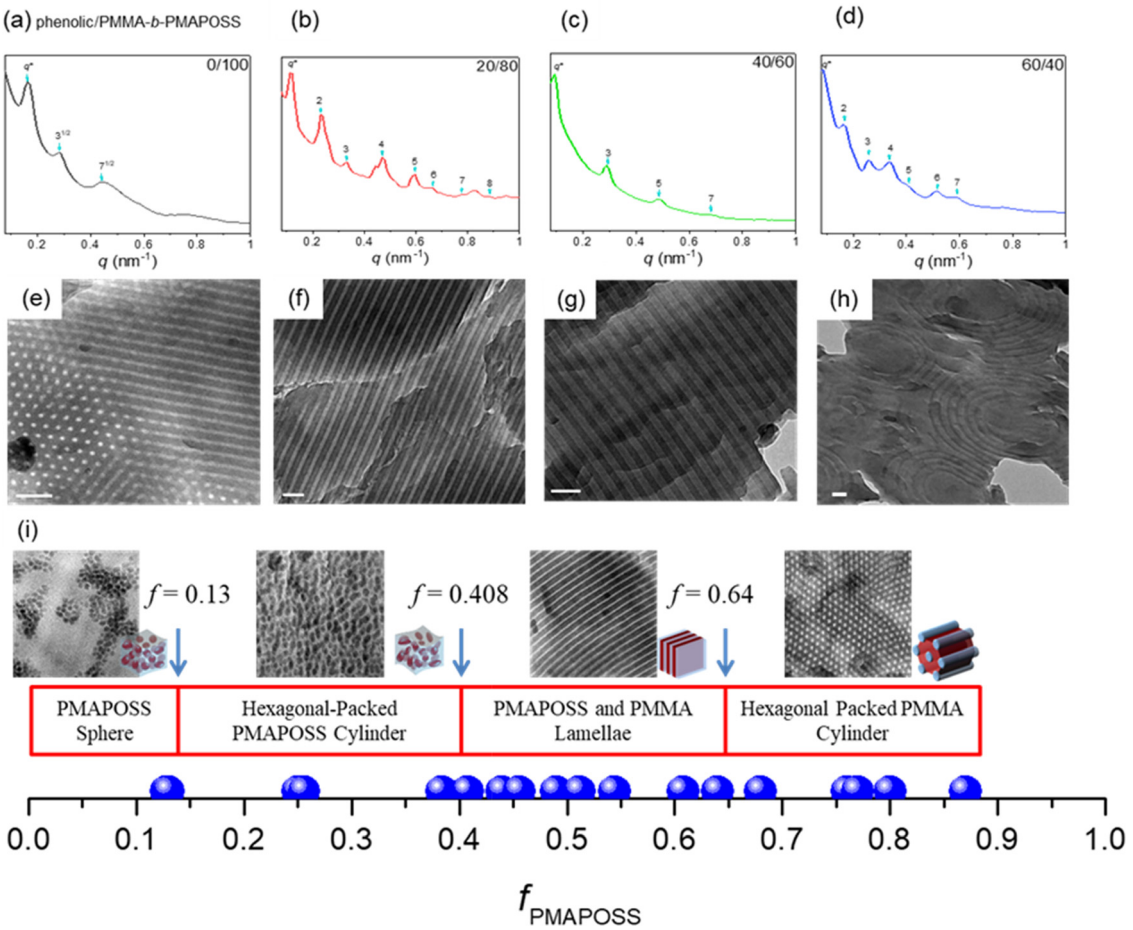


Fig. 17 (a–d) SAXS and (e–h) TEM analyses of phenolic/PMA-*b*-PMAPOSS blends: (a and e) 0/100, (b and f) 20/80, (c and g) 40/60, (d and h) 60/40. (i) Corresponding phase diagram with various PMAPOSS volume fractions.[134] Reproduced from ref. 134 with permission from American Chemical Society.

lengths. Interestingly, upon self-assembly in solution, when the content of POSS moieties was increased in the BCPs, the size of the micelles increased (Fig. 20).[140] He *et al.* used ATRP with PDMS-Br as the macroinitiator to prepare three different diblock and triblock copolymers: PDMS-*b*-PMMA, PDMS-*b*-PMMA-*b*-PMAPOSS, and PDMS-*b*-PMMA-*b*-PDFHM; they then examined the effects of PMAPOSS and PDFHM on the thermal stability and surface hydrophilicity of these copolymers. The presence of PDFHM and PMAPOSS in the triblock copolymers improved the dynamic dewetting and hexadecane-dewetting characteristics, respectively. In addition, the thermal stability of these copolymers improved upon incorporation of PMAPOSS or PDFHM into the PDMS-*b*-PMMA structure.[141] Zhang and co-workers used one-pot RAFT polymerization to prepare PS-*b*-MIPOSS alternating copolymers and BCPs of low polydispersity index (PDI) and high DP. TEM images of these materials revealed different self-assembled structures arising from the presence of the POSS spheres, with a transition from HPC to LAM structures in the bulk state when the MIPOSS content was increased from 13 to 64%.[142]

### Self-assembly of di-functionalized POSS NPs

Di-functionalized POSS cages are generally synthesized using two approaches. The first involves the precise hydrolysis of OV-POSS to form *ortho*, *meta*, and *para* di-functionalized POSS NPs; these POSS cages must be separated and purified chromatographically.[143] The Dong group used a precise and efficient exponential growth method to construct a new type of discrete giant polymeric chains based on POSS NPs, with different region-configurations, surface functionalities, compositions, and sizes. Based on SAXS analyses (Fig. 21), the self-assembly of the amphiphilic *p*-C$_n$D block chains resulted in HPC and LAM lattices upon increasing the volume fraction of the hydrophobic segments.[144]

Zhang *et al.* synthesized various mixed [6 : 2] hetero-arm star polymers on the POSS cubic scaffold. They introduced six PS arms and two PCL chains; ROP of two OH groups produced the two PCL chains, while six vinyl groups were converted to $N_3$ units for the grafting of PS chains onto the POSS cage (Fig. 22).[145] They also reported a double chain giant surfactant by using these mixed di-functionalized POSS cages with six

 

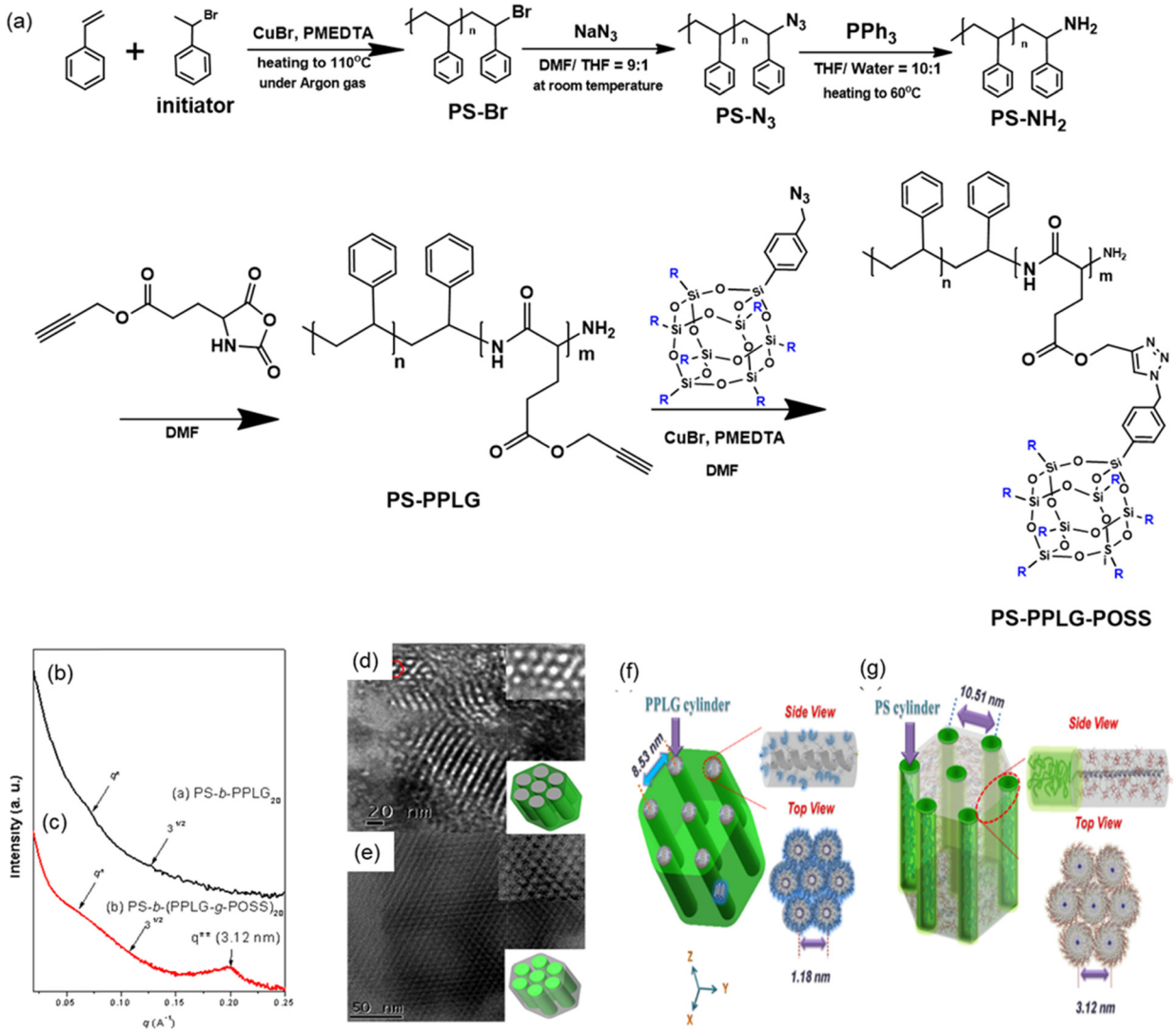


Fig. 18 (a) Synthesis of PS-*b*-(PPLG-*g*-POSS) using a combination of ATRP, NCA-ROP, and click reactions of PS-*b*-PPLG with mono-functionalized $N_3$-POSS. (b and c) SAXS patterns, (d and e) TEM images, and (f and g) schematic representations of the self-assembled structures of (b, d and f) PS-*b*-PPLG and (c, e and g) PS-*b*-(PPLG-*g*-POSS) diblock copolymers.[135] Reproduced from ref. 135 with permission from the Royal Society of Chemistry.

OH-functionalized POSS heads and two PS tails tethered at the ortho, meta, and para position of the POSS cube [Fig. 23(a)]. Using SAXS and TEM, they observed an order-order morphological transitions for the *meta*-isomer (from an LAM to DG structure) [Fig. 23(b) and (c)] and *ortho*-isomer (from a DG to HPC structure) [Fig. 23(d)] upon increasing the temperature, because of differences in the free energy contributions as arising from head-to-head POSS interactions, the entropy of the PS tails, and the interfacial energy. Fig. 23(d) summarizes the phase diagrams of these double chain giant surfactants based on POSS cages.[146]

Using this approach, the synthesis of di-functionalized POSS cages is quite complicated and time consuming. A more practical approach is the relatively simple synthesis of di-functionalized POSS cages from difunctional double-decker silsesquioxanes (DDSQs) [Fig. 24(a)].[147] This approach allows the ready preparation of di-functionalized POSS compounds through hydrosilylation with alkenes or alkynes. For example, we used DDSQ-VBC [Fig. 24(b)] as the macro-initiator for ATRP to prepare two main-chain BCPs, PVPh-*b*-PS [Fig. 24(e)] and P4VP-*b*-PS [Fig. 24(f)], featuring hydrogen bond donor (PVPh) and acceptor (P4VP) segments. TEM revealed that the PS-*b*-P4VP and PS-*b*-PVPh main-chain-type BCPs based on DDSQ formed spherical, HCP, and LAM structures [Fig. 24(g)–(l)].[147]

We have observed mesoporous FK phases in the self-assembled structures obtained from di-functionalized DDSQ.[148] We prepared phenolic/DDSQ hybrids featuring various amounts of DDSQ from the reactions of phenol, DDSQ-4OH, and $CH_2O$ in NaOH medium [Fig. 25(a)].[149] Because of the high thermal stability of these phenolic/DDSQ hybrids, we obtained a new

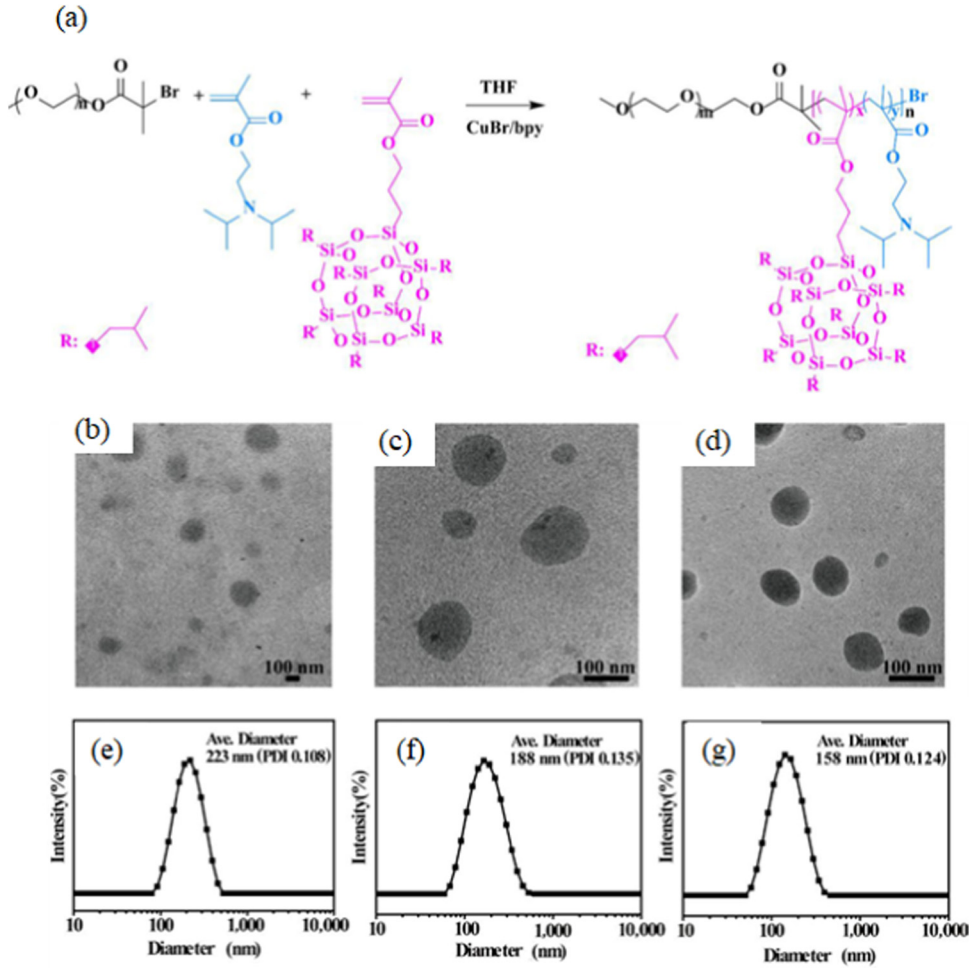


Fig. 19 (a) Synthesis of PEG-*b*-P(MAPOSS-*co*-DPA) through ATRP. (b–d) TEM images and (e–g) DLS analyses of various MAPOSS compositions in corresponding BCPs: (b and e) BCP1, (c and f) BCP2, and (d and g) BCP3.[138] Reproduced from ref. 138 with permission from American Chemical Society.

way to prepare mesoporous FK phases—through templating with the PEO-*b*-PCL diblock copolymer [Fig. 25(b) and (c)]. Fig. 25(d)–(g) display corresponding TEM images revealing the various FK phases, including σ, A15, H, and Z phases, obtained upon increasing the DDSQ composition in the phenolic/DDSQ hybrids, as well as the phase diagram of these mesoporous structures.[149] Interestingly, Cheng *et al.* studied and examined the self-assembly behaviors of three binary systems, PBI/CPBI, BTA1/CPBI, and BTA2/CPBI and they found that a series of unusual superlattices observations including quasi-F–K phases, $NaZn_{13}$, $CaCu_5$, and $MgZn_2$ phase.[150] The same group prepared multibranched giant molecules named OP8 and OP14 *via* tethering eight and fourteen aliphatic isooctyl-OPOSS cages. Then, azide-alkyne [3+2] cycloaddition for connecting the core and cages. They found that the binary mixtures of OP8/OP14 with mass ratio = 1/2 displayed DQC, DDQC, and Frank–Kasper σ structures during thermal annealing.[151] Recently, Zhang's group constructed a series of multi-tailed $B_2AB_2$ giant surfactant materials containing POSS and PS as hydrophobic tails through click reaction. Interestingly, the phase structure of $B_2AB_2$ depends on the regio-configuration of these materials. For example, the *meta*- and *para* isomers showed HEX phase and the *ortho*-isomer formed metastable DQC phase.[152]

Recently, porous organic polymers (POPs) have been attracting much attention because they possess high surface areas, low densities, high chemical and thermal stabilities, and tunable porosities; they can be classified into hypercrosslinked polymers, covalent organic frameworks, covalent triazine frameworks, and conjugated microporous polymers.[153–163] These POPs have a diverse range of applications in energy storage, gas capture and separation, photocatalysis, $H_2$ evolution, and optical devices. Incorporating DDSQ or POSS into organic polymers to form self-assembled and ordered structures is also of interest when preparing porous organic/inorganic microporous polymers (POIPs).[164–167] We have used Sonogashira–Hagihara coupling of DDSQBr with tetraphenylethene (TPE) and carbazole (Car) derivatives to append TPE and Car units, respectively, onto DDSQ moieties for the preparation of POIPs. These two POIPs exhibited high thermal

 

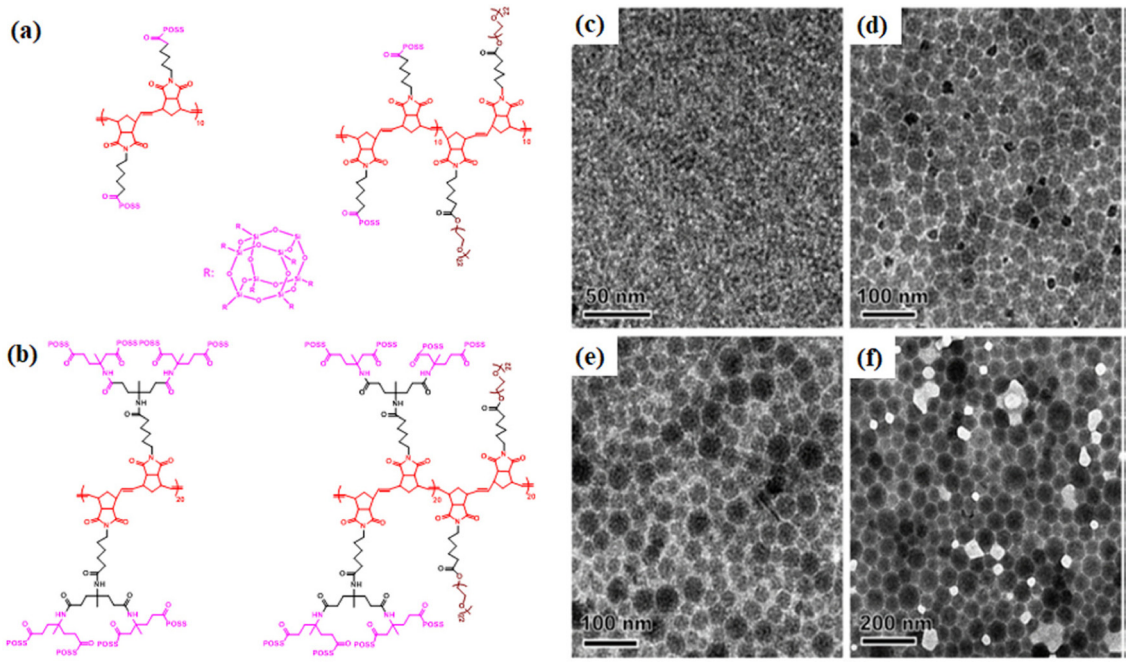


Fig. 20 (a) Synthesis of polynorbornenes composed of side chains featuring one to four POSS cages. (b) Corresponding poly(*N*-*n*POSS)$_m$-*b*-poly(*N*-PEO)$_p$ BCPs featuring a bottlebrush polynorbornene with side chains of PEO units, where *n* is number of POSS cages as side chains and *m* and *p* are the degrees of polymerization of each block segment. (c–f) TEM images of (c) poly(*N*-1POSS)$_{20}$-*b*-poly(*N*-PEO)$_{20}$, (d) poly(*N*-2POSS)$_{20}$-*b*-poly(*N*-PEO)$_{20}$, (e) poly(*N*-3POSS)$_{20}$-*b*-poly(*N*-PEO)$_{20}$, and (f) poly(*N*-4POSS)$_{20}$-*b*-poly(*N*-PEO)$_{20}$.[140] Reproduced from ref. 140 with permission from the Royal Society of Chemistry.

stability, with a high char yield (*ca.* 77.4 wt%) and high specific capacitance for the Car-DDSQ POIP.[88]

### Self-assembly of multi-functionalized POSS NPs

The syntheses of multi-functionalized POSS cages are generally performed using two methods: (i) hydrolysis and condensation of trichlorosilane ($HSiCl_3$) or trialkoxylsilanes [$HSi(OR)_3$], in low yield (*ca.* 10 wt%), and (ii) hydrosilylation of various alkenes or alkynes using $(HSiO_{1.5})_8$ or $Q_8M_8^H$ $(HMe_2SiOSiO_{1.5})_8$ and Pt catalysts, in very high yield (*ca.* 90 wt%) [Fig. 1(C)].[85,168]

We have used hydrosilylation, click, and condensation reactions to synthesize various octa-functionalized benzoxazine (BZ) POSS cage structures.[169] The resulting octa-functionalized polybenzoxazine (PBZ)/POSS derivatives displayed improved thermal and mechanical properties, because the POSS cages hindered the chain mobility of the PBZ structures.[169] We have also prepared octa-functionalized BZ-POSS derivatives through supramolecular interactions (multiple hydrogen bonds) between octa-functionalized adenine (A)-POSS [Fig. 26(b)] and thymine (T)-functionalized BZ [Fig. 26(a)],[170] stabilized through multiple A–T binary pairs in the OA-POSS/T-BZ hybrids.[170] TEM images [Fig. 26(c)] revealed that this T-BZ/OA-POSS hybrid self-assembled into a LAM structure as a result of strong multiple A–T hydrogen bonding.[171] We also synthesized an octa-functionalized diamidopyridine POSS (OD-POSS) and blended it with mono- and di-uracil (U)-functionalized PEG.[172] Through multiple D–U hydrogen bonding interactions (Fig. 27), the resulting POSS-based supramolecular polymers exhibited improved thermal properties and self-assembled into spherical structures, as observed using TEM.

Star BCPs based on POSS cages have also been investigated widely in recent years.[173–176] Zhang *et al.* prepared a star-shaped PCL-*b*-PDMAEM BCP based on POSS cages; TEM and DLS revealed that it self-assembled into unimolecular micelles.[177] Singha *et al.* used a combination of ROP and RAFT polymerization to synthesize a star-shaped PCL-*b*-PGLC BCP based on POSS cages; it self-assembled into core–shell structures, as revealed by TEM and SEM imaging.[178] He *et al.* used RAFT polymerization for the thermogelling of POSS with a star-shaped PDMAEMA-*b*-PNIPAm BCP. They examined the sol–gel transitions, structures, and rheology of the resulting copolymers, and found that these copolymers could self-assemble into microgels when heating dilute aqueous solutions.[179] We have synthesized various star PS-*b*-P4VP and PS-*b*-PVPh diblock copolymers based on POSS cages (Fig. 28); TEM and SAXS revealed that they could form self-assembled LAM structures.[180] Furthermore, Dong *et al.* prepared a library of amphiphilic patchy clusters based on POSS cages with accurate surface and symmetry properties using different chemical reactions (click, esterification, and thiol–ene reactions). They revealed that these POSS patchy clusters could be formed in various nanostructures, dodecagonal quasicrystalline phase (DQC), and Frank–Kasper σ phase, respectively, by controlling and tunable the molecular symmetry and composition.[181]

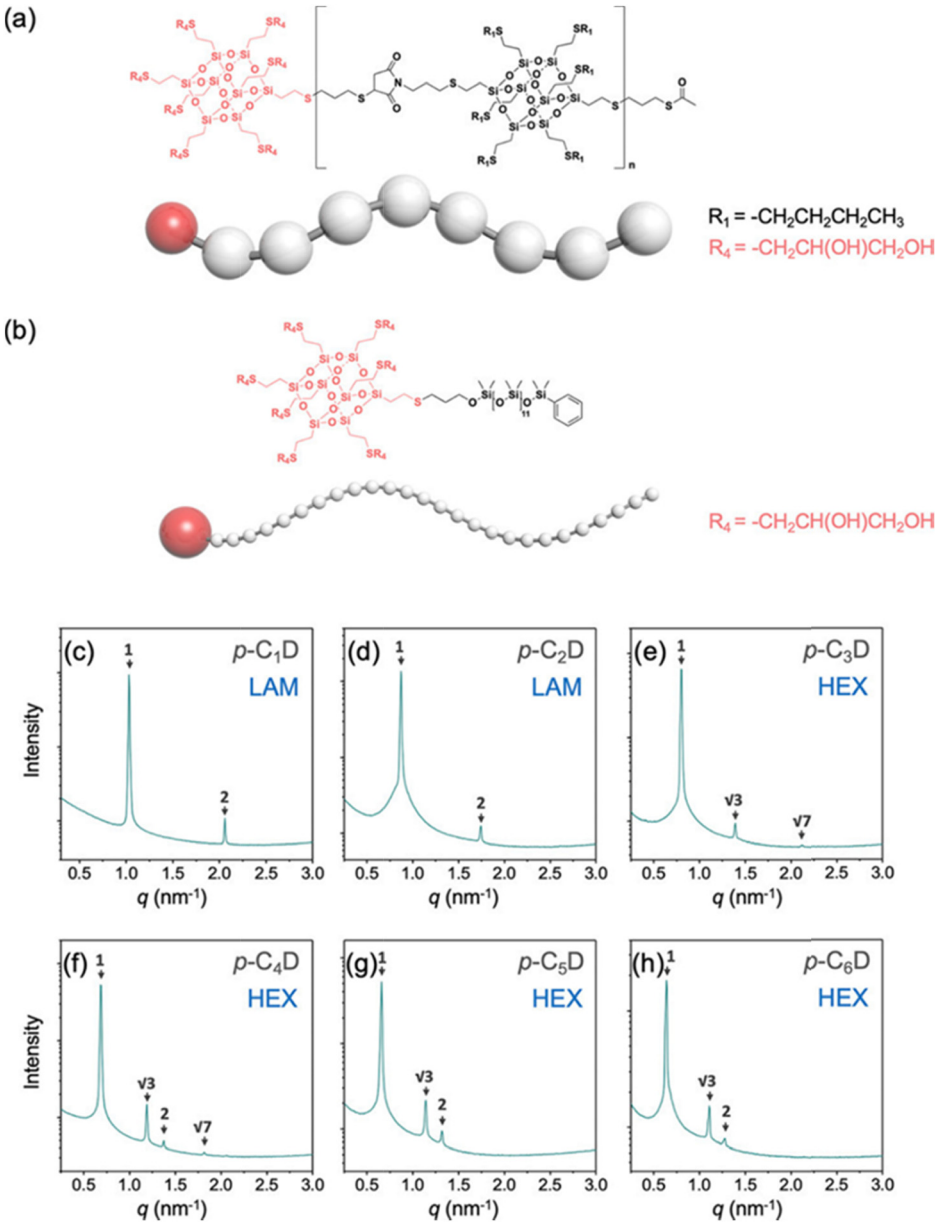


Fig. 21 (a) Chemical structure of $p$-C$_n$D based on amphiphilic POSS BCP. (b) Corresponding counterpart of $S_{13}$D. (c–h) SAXS analyses performed at various compositions of $p$-C$_n$D.[144] Reproduced from ref. 144 with permission from American Chemical Society.

## Conclusions and future outlook

The POSS cage is the smallest possible silica NP that can be used to form hybrid materials with polymer matrices. The resulting polymer/POSS hybrids can form unique self-assembled structures—ones that have not been observed for other polymer/silica hybrids, formed using, for example, PDMS and clay. Accordingly, POSS materials have attracted significant attention in recent years. In this Review, we discuss recent progress in the self-assembly of organic/inorganic POSS hybrids derived from mono-, di-, and multi-functionalized POSS cages, with a focus on the thermal properties and secondary structures of these polymer/POSS hybrids. Although great progress has been made in preparing POSS hybrids with many applications. Many challenges remain such as preparation giant materials with fractal and DQC structures and synthesis of high crystalline COF materials based on POSS for solar cell, drug delivery, optoelectronic devices, hydrogen, and oxygen production. In the near future, we expect that new POSS hybrid materials having self-assembled mesoporous or microporous structures will be of great interest because the POSS building block should provide new opportunities to prepare organic/inorganic porous materials (*e.g.*, COFs and CMPs). Furthermore, the synthesis of polymer/POSS hybrids displaying new FK phases remains another challenge, with explorations of this field almost certain to reveal new and beneficial properties.

 

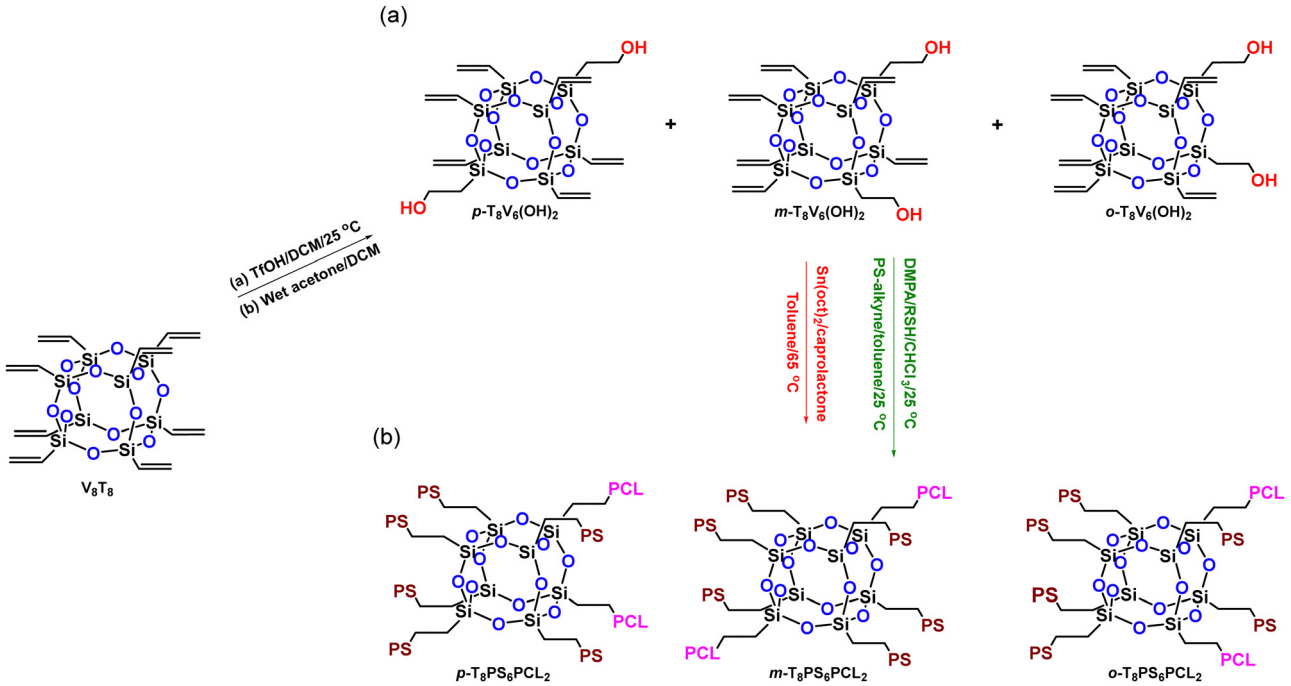


Fig. 22 (a) Synthesis of di-functionalized POSS cages through the precise hydrolysis of OV-POSS to form *ortho*, *meta*, and *para* substituted OV-POSS-2OH. (b) Synthesis of various mixed [6 : 2] hetero-arm star polymers on the POSS cube, with six PS arms and two PCL chains formed through ROP and click reactions.[143,145] Reproduced from ref. 143 with permission from Wiley-VCH. Reproduced from ref. 145 with permission from the Royal Society of Chemistry.

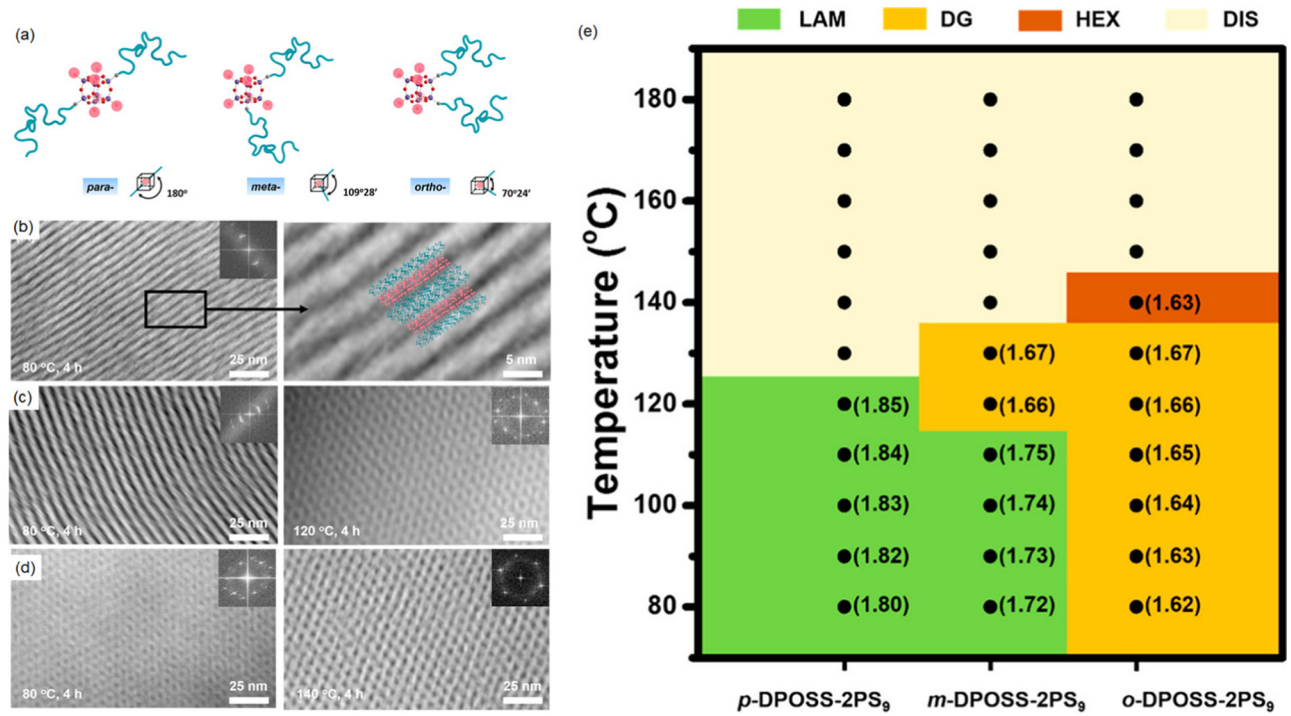


Fig. 23 (a) Chemical structures of six di-functionalized POSS cages with six OH-functionalized POSS heads and two PS tails tethered at *ortho*, *meta*, and *para* positions. (b–d) TEM images of (b) the *meta* isomer after thermal annealing at 80 °C for 4 h; (c) the *meta* isomer after thermal annealing at 80 °C for 4 h (left) and 120 °C for 4 h (right); and (d) the *ortho* isomer after thermal annealing at 80 °C for 4 h (left) and 140 °C for 4 h (right). (e) Full phase diagram of these double-chain giant surfactants.[146] Reproduced from ref. 146 with permission from American Chemical Society.

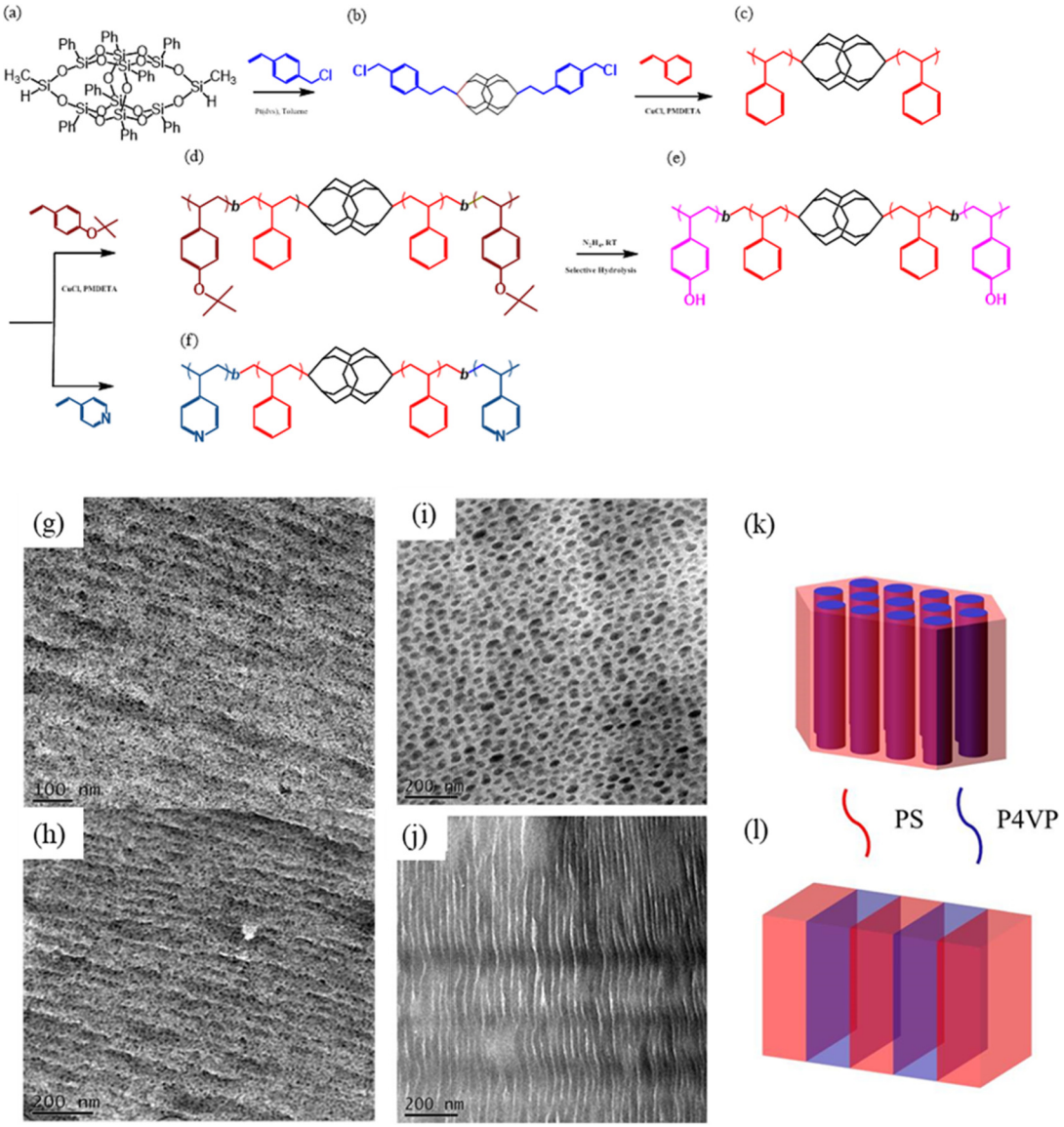


Fig. 24 (a–f) Synthesis of main-chain-type diblock copolymers based on DDSQ cages: (a) DDSQ; (b) DDSQ-VBC initiator; (c) PS formed through ATRP; (e) PS-*b*-PVPh formed through sequential ATRP and hydrolysis of (d) PS-*b*-PtBuOS and (f) PS-*b*-P4VP. (g, i and j) TEM images and (h, k and l) corresponding self-assembled structures of (g and h) PS-*b*-PVPh and (i and k) $PS_{91}$-*b*-$P4VP_{62}$ (HPC structure) and (j and l) $PS_{91}$-*b*-$P4VP_{98}$ (LAM structure).[147] Reproduced from ref. 147 with permission from MDPI.

 

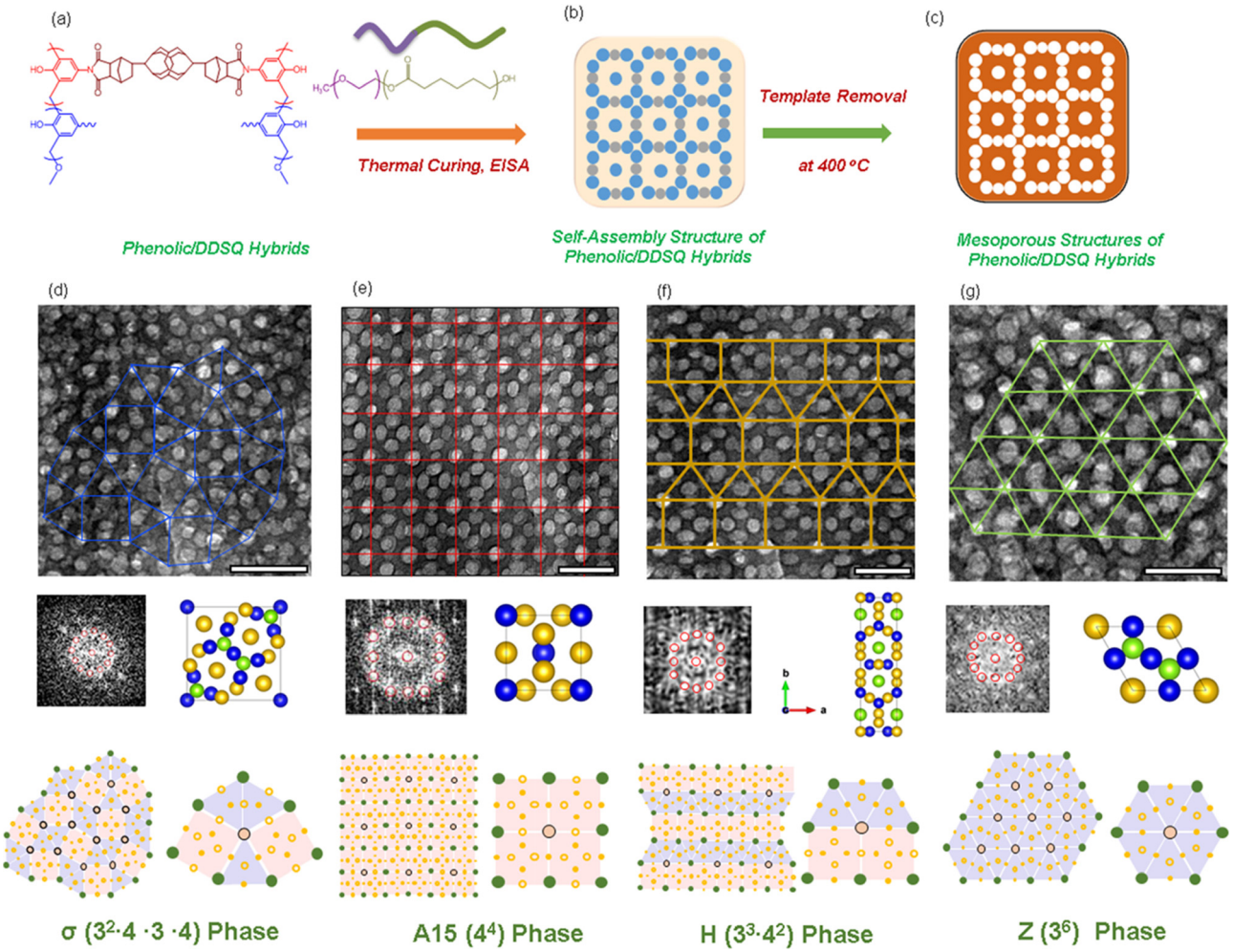


Fig. 25 (a) Chemical structures of phenolic/DDSQ hybrids. (b) Self-assembled structure templated by the PEO-*b*-PCL diblock copolymer. (c) Mesoporous phenolic/DDSQ hybrids obtained after removal of the template. (d–g) TEM and FFT analyses of corresponding mesoporous phenolic/DDSQ structures featuring FK phases, based on the PDDSQ-*x*/PEO-*b*-PCL = 80/20 blend: (d) σ phase from PDDSQ-20 with $3^2{\cdot}4{\cdot}3{\cdot}4$ tiling number, (e) A15 phase from PDDSQ-30 with $4^4$ tiling number, (f) H phase from PDDSQ-50 with $3^3{\cdot}4^2$ tiling number, and (g) Z phase from PDDSQ-80 with $3^6$ tiling number.[149] Reproduced from ref. 149 with permission from Wiley-VCH.

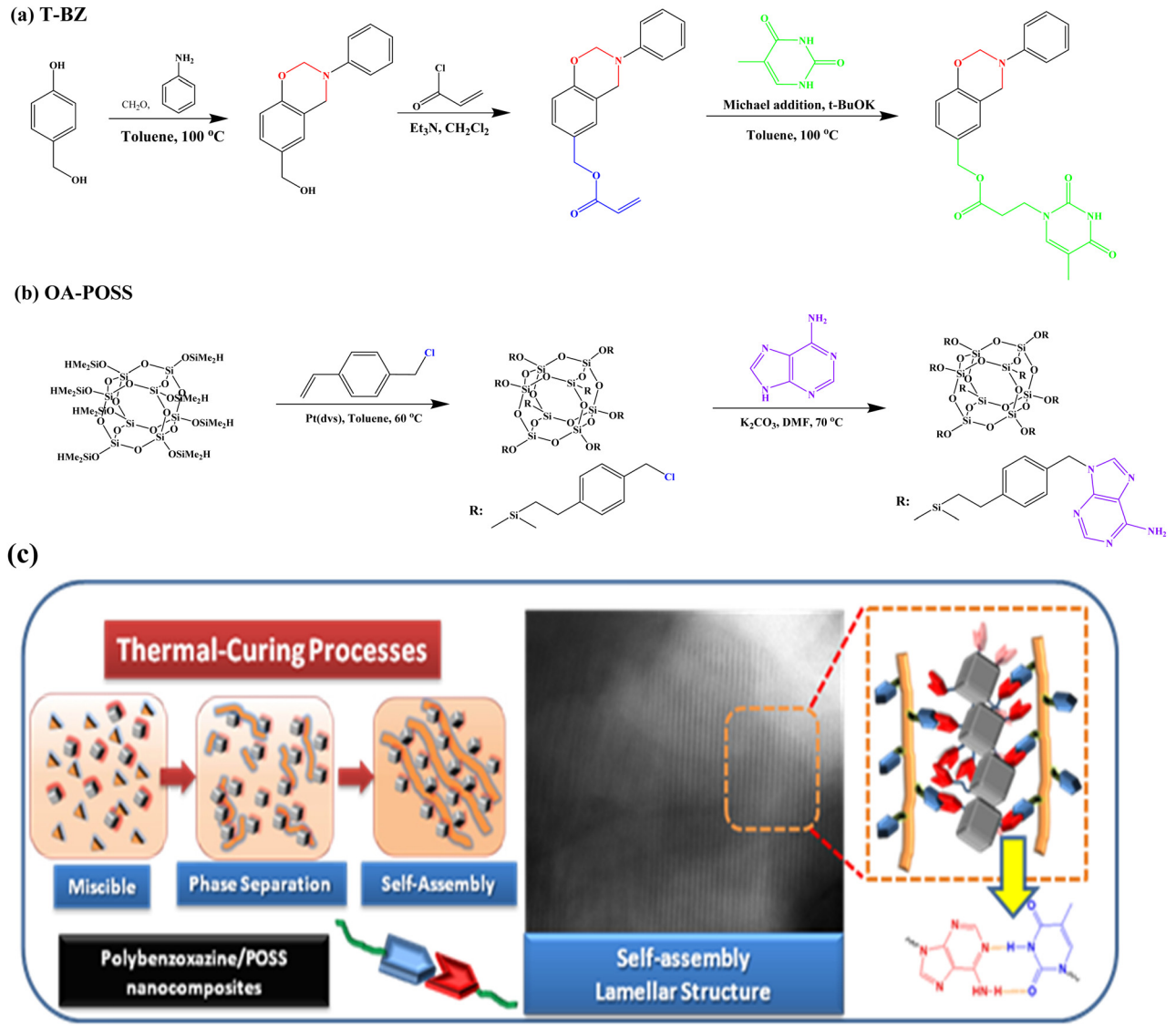


Fig. 26 (a and b) Chemical structures and synthesis of (a) thymine-functionalized BZ (T-BZ) and (b) OA-POSS. (c) TEM image recorded after the thermal curing of T-BZ/OA-POSS hybrids having a LAM structure, stabilized through multiple A–T hydrogen bonds.[170,171] Reproduced from ref. 170 with permission from the Royal Society of Chemistry. Reproduced from ref. 171 with permission from American Chemical Society.

## Abbreviation

| | |
|---|---|
| ATRP | Atom transfer radical polymerization |
| DDSQ | Double-deckered silsesquioxanes |
| DSC | Differential scanning calorimetry |
| FTIR | Fourier transform infrared spectroscopy |
| NCA | *N*-Carboxyanhydride |
| NMRP | Nitroxide mediated radical polymerization |
| PCL | Poly(caprolactone) |
| PDMS | Poly(dimethyl siloxaine) |
| PEG | Poly(ethylene glycol) |
| PFS | Poly(ferrocenyl dimethylsilane) |
| PS | Polystyrene |
| PMMA | Poly(methyl methacrylate) |
| PMDETA | Pentamethyl diethylenetriamine |
| PVP | Poly(vinyl pyrrolidone) |
| PVPh | Poly(vinyl phenol) |
| PVPh-*co*-PVP-POSS | Poly(hydroxystyrene-*co*-vinylpyrrolidone-*co*-isobutylstyryl polyhedral oligosilsesquioxanes) |
| PBLG | Poly(γ-benzyl-L-glutamate) |
| BTA | Benzene-1,3,5-tricarboxamide |
| ROP | Ring-opening polymerization |
| PBZ | Polybenzoxazine |
| RAFT | Reversible addition-fragmentation chain transfer |
| LB | Langmuir-Blodgett |
| DQC | Decagonal quasicrystal |
| SAXS | Small angle X-ray scattering |

 

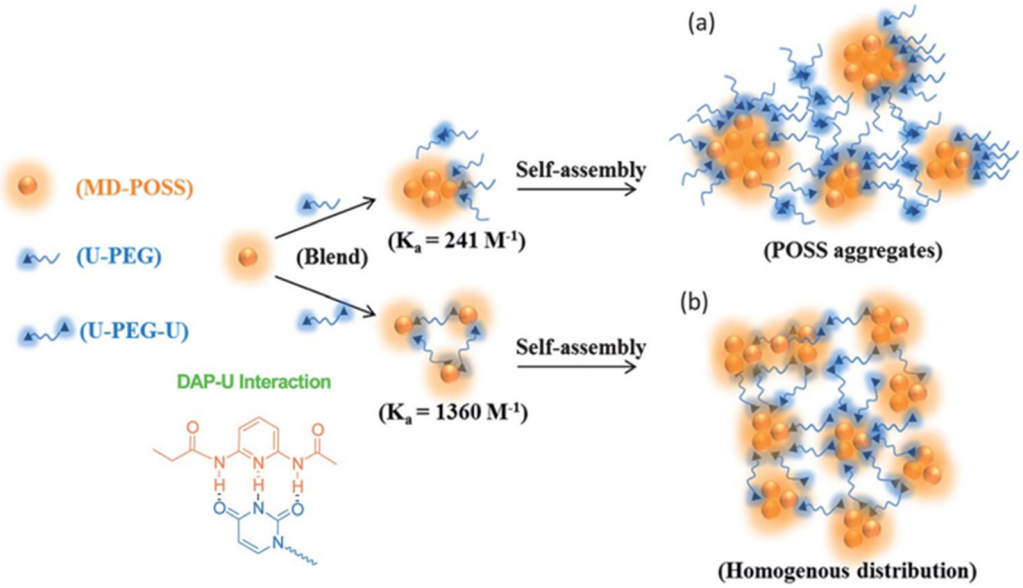


Fig. 27 Possible self-assembled structures and multiple hydrogen bonding interactions in (a) MD-POSSS/U–PEG and (b) MD-POSS/U–PEG–U hybrids.[172] Reproduced from ref. 172 with permission from the Royal Society of Chemistry.

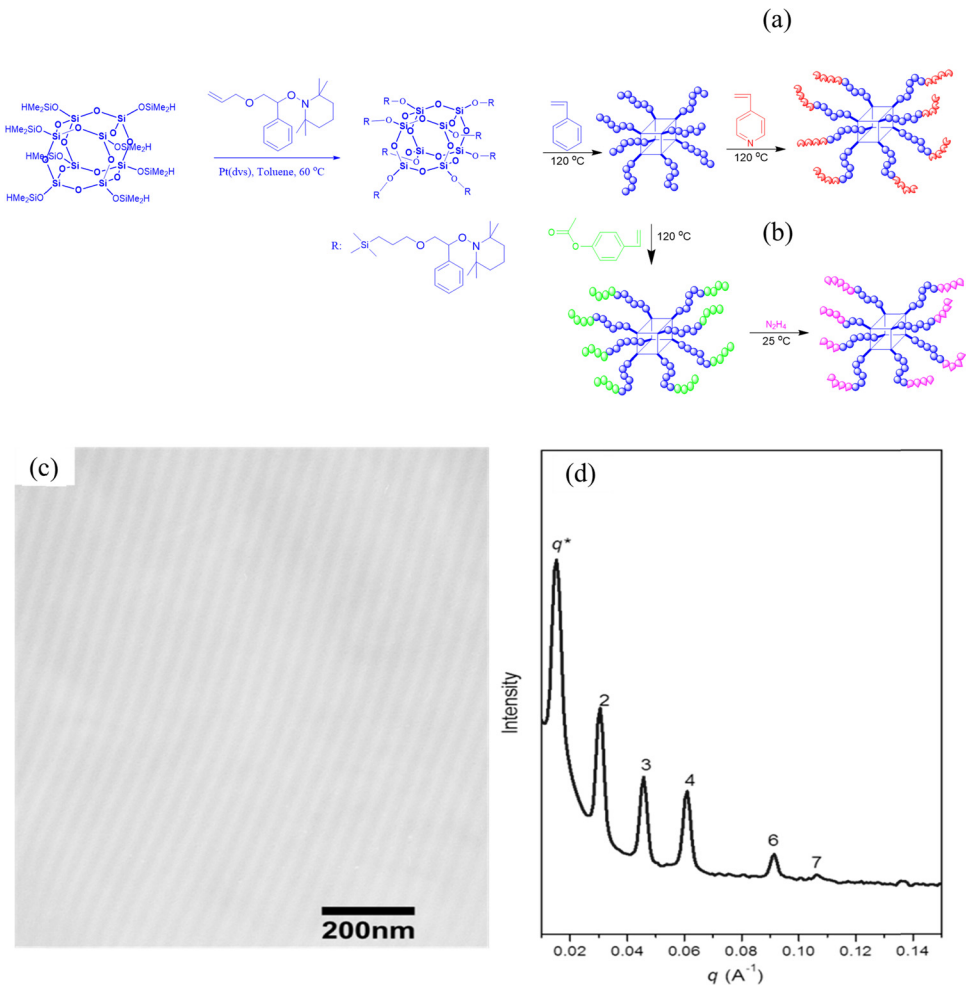


Fig. 28 (a and b) Synthesis of star-shaped (a) PS-*b*-P4VP through NMP and (b) PS-*b*-PVPh diblock copolymers through NMP and hydrolysis, based on POSS cages. (c) TEM and (d) SAXS analyses of the star-shaped PS-*b*-P4VP diblock copolymer having a LAM structure.[180] Reproduced from ref. 180 with permission from Wiley-VCH.

| | |
|---|---|
| SEM | Scanning electron microscopy |
| TEM | Transmission electron microscopy |
| $T_g$ | Glass transition temperature |
| WAXD | Wide angle X-ray diffraction |

## Conflicts of interest

The authors declare no competing financial interest.

## Acknowledgements

This study was supported financially by the Ministry of Science and Technology, Taiwan, under contracts MOST 108-2221-E-110-014-MY3, 109-2221-E-110-067-MY3, and 111-2223-E-110-004.

## References

1 W. J. Zhang, C. Y. Hong and C. Y. Pan, *Macromol. Rapid Commun.*, 2019, **40**, 1800279.
2 T. C. Tseng and S. W. Kuo, *Macromolecules*, 2018, **51**, 6451–6459.
3 S. Alexandris, A. Franczyk, G. Papamokos, B. Marciniec, K. Matyjaszewski, K. Koynov, M. Mezger and G. Floudas, *Macromolecules*, 2015, **48**, 3376–3385.
4 J. Zhu and R. C. Hayward, *J. Am. Chem. Soc.*, 2008, **130**, 7496–7502.
5 H. Miyase, Y. Asai, A. Takano and Y. Matsushita, *Macromolecules*, 2017, **50**, 979–986.
6 C. T. Tsou and S. W. Kuo, *Macromolecules*, 2019, **52**, 8374–8383.
7 M. G. Mohamed, E. C. Atayde Jr, B. M. Matsagar, J. Na, Y. Yamauchi, K. C.-W. Wu and S. W. Kuo, *J. Taiwan Inst. Chem. Eng.*, 2020, **112**, 180–192.
8 S. W. Kuo, *Polym. Interact.*, 2022, **71**, 393–410.
9 E. L. Lin, W. L. Hsu and Y. W. Chiang, *ACS Nano*, 2018, **12**, 485–493.
10 X. Y. Yan, Q. Y. Guo, X. Y. Liu, Y. Wang, J. Wang, Z. Su, J. Huang, F. Bian, H. Lin, M. Huang, Z. Lin, T. Liu, Y. Liu and S. Z. D. Cheng, *J. Am. Chem. Soc.*, 2021, **143**, 21613–21621.
11 E. Verde-Sesto, A. Arbe, A. J. Moreno, D. Cangialosi, A. Alegría, J. Colmeneroa and J. A. Pomposo, *Mater. Horiz.*, 2020, **7**, 2292–2313.
12 P. Bačová, R. Foskinis, E. Glynos, A. N. Rissanou, S. H. Anastasiadis and V. Harmandaris, *Soft Matter*, 2018, **14**, 9562–9570.
13 P. Bačová, E. Glynos, S. H. Anastasiadis and V. Harmandaris, *ACS Nano*, 2019, **13**, 2439–2449.
14 Y. Y. Huang, J. Y. Hsu, H. L. Chen and T. Hashimoto, *Macromolecules*, 2007, **40**, 3700–3707.
15 S. C. Tsai, Y. C. Lin, E. L. Lin, Y. W. Chiang and S. W. Kuo, *Polym. Chem.*, 2016, **7**, 2395–2409.
16 A. F. M. EL-Mahdy, T. C. Yu, M. G. Mohamed and S. W. Kuo, *Macromolecules*, 2021, **54**, 1030–1042.
17 T. Asari, S. Arai, A. Takano and Y. Matsushita, *Macromolecules*, 2006, **39**, 2232–2237.
18 S. W. Kuo, *Polym. Intercat.*, 2009, **58**, 455–464.
19 S. Song, H. Zhou, I. Manners and M. A. Winnik, *Chem*, 2021, **7**, 2800–2821.
20 F. R. Xu, R. Shi, X. M. Jia, S. C. Chai, H. L. Li, H. J. Qian and Z. Y. Lu, *Soft Matter*, 2021, **17**, 5897–5906.
21 M. Watanabe, Y. Asai, J. Suzuki, A. Takano and Y. Matsushita, *Macromolecules*, 2020, **53**, 10217–10224.
22 A. B. Chang and F. S. Bates, *ACS Nano*, 2020, **14**, 11463–11472.
23 B. A. Lindquist, R. B. Jadrich, W. D. Pineros and T. M. Truskett, *J. Phys. Chem. B*, 2018, **122**, 5547–5556.
24 K. K. Lachmayr and L. R. Sita, *Angew. Chem., Int. Ed.*, 2020, **59**, 3563–3567.
25 H. J. Sun, S. Zhang and V. Percec, *Chem. Soc. Rev.*, 2015, **44**, 3900–3923.
26 M. Huang, K. Yue, J. Wang, C.-H. Hsu, L. Wang and S. Z. D. Cheng, *Sci. China: Chem.*, 2018, **61**, 33–45.
27 S. Lee, C. Leighton and F. S. Bates, *Proc. Natl. Acad. Sci. U. S. A.*, 2014, **111**, 17723–17731.
28 A. Reddy, M. B. Buckley, A. Arora, F. S. Bates, K. D. Dorfman and G. M. Grason, *Proc. Natl. Acad. Sci. U. S. A.*, 2018, **115**, 10233–10238.
29 X. Feng, C. J. Burke, M. Zhuo, H. Guo, K. Yang, A. Reddy, I. Prasad, R. M. Ho, A. Avgeropoulos, G. M. Grason and E. L. Thomas, *Nature*, 2019, **575**, 175–179.
30 A. Jangizehi, F. Schmid, P. Besenius, K. Kremer and S. Seiffert, *Soft Matter*, 2020, **16**, 10809–10859.
31 A. F. M. EL-Mahdy, T. C. Yu and S. W. Kuo, *Chem. Eng. J.*, 2021, **414**, 128796.
32 C. J. Hsu, C. W. Tu, Y. W. Huang, S. W. Kuo, R. H. Lee, Y. T. Liu, H. Y. Hsueh, J. Aimi and C. F. Huang, *Polymer*, 2021, **213**, 123212.
33 C. Zhang, P. Xiao, F. Ni, J. Gu, J. Chen, Y. Nie, S. W. Kuo and T. Chen, *Chem. Eng. J.*, 2022, **428**, 131142.
34 B. M. Yavitt, D. Salatto, Y. Zhou, Z. Huang, L. iegart, V. Bocharova, A. E. Ribbe, A. P. Sololov, K. S. Schweizer and T. Koga, *ACS Nano*, 2021, **15**, 11501–11513.
35 S. Parvate, J. Singh, P. Dixit, J. R. Vennapusa, T. K. Maiti and S. Chattopadhyay, *ACS Appl. Polym. Mater.*, 2021, **3**, 1866–1879.
36 M. Ibrahim, N. Begam, V. Padmanabhan and J. K. Basu, *Soft Matter*, 2018, **14**, 6076–6082.
37 M. G. Mohamed, M. M. Samy, T. H. Mansoure, S. U. Sharma, M. S. Tsai, J. H. Chen, J. T. Lee and S. W. Kuo, *ACS Appl. Energy Mater.*, 2022, **5**, 3677–3688.
38 J. Zhou, X. Zhang, S. Zhao, C. Ye, Z. Zhang, S. W. Kuo and Z. Xin, *Polymer*, 2022, **244**, 124561.
39 M. M. Samy, M. G. Mohamed, A. F. M. EL-Mahdy, T. H. Mansoure, K. C. W. Wu and S. W. Kuo, *ACS Appl. Mater. Interfaces*, 2021, **13**, 51906–51916.
40 Z. Lin, X. Yang, H. Xu, T. Sakurai, W. Matsuda, S. Seki, Y. Zhou, J. Sun, K.-Y. Wu, X.-Y. Yan, R. Zhang, M. Huang, J. Mao, C. Wesdemiotis, T. Aida, W. Zhang and S. Z. D. Cheng, *J. Am. Chem. Soc.*, 2017, **139**, 18616–18622.
41 C.-L. Wang, W.-B. Zhang, H.-J. Sun, R. M. Van Horn, R. R. Kulkarni, C.-C. Tsai, C.-S. Hsu, B. Lotz, X. Gong and S. Z. D. Cheng, *Adv. Energy Mater.*, 2012, **2**, 1375–1382.

 

42 X. H. Zheng, J. F. Zhao, T. P. Zhao, T. Yang, X. K. Ren, C. Y. Liu, S. Yang and E. Q. Chen, *Macromolecules*, 2018, **51**, 4484–4493.
43 L. A. Connal, N. A. Lynd, M. J. Robb, K. A. See, S. G. Jang, J. M. Spruell and C. J. Hawker, *Chem. Mater.*, 2012, **24**, 4036–4042.
44 C. Chen, Z. Xiao and L. A. Connal, *Aust. J. Chem.*, 2016, **69**, 741–745.
45 J. Wang, W. Li and J. Zhu, *Polymer*, 2014, **55**, 1079–1096.
46 B. Sarkar and P. Alexandridis, *Prog. Polym. Sci.*, 2015, **40**, 33–62.
47 M. Stefik, S. Guldin, S. Vignolini, U. B. Wiesner and U. Steiner, *Chem. Soc. Rev.*, 2015, **44**, 5076–5091.
48 C. J. Mable, R. R. Gibson, S. Prevost, B. E. McKenzie, O. O. Mykhaylyk and S. P. Armes, *J. Am. Chem. Soc.*, 2015, **137**, 16098–16108.
49 I. Villaluenga, X. C. Chen, D. Devaux, D. T. Hallinan and N. P. Balsara, *Macromolecules*, 2015, **48**, 358–364.
50 B. J. Kim, J. Bang, C. J. Hawker and E. J. Kramer, *Macromolecules*, 2006, **39**, 4108–4114.
51 B. J. Kim, G. H. Fredrickson and E. J. Kramer, *Macromolecules*, 2008, **41**, 436–447.
52 Y. C. Lin and S. W. Kuo, *J. Polym. Sci., Part A: Polym. Chem.*, 2011, **49**, 2127–2137.
53 R. Goseki, A. Hirao, M. Kakimoto and T. Hayakawa, *ACS Macro Lett.*, 2013, **2**, 625–629.
54 K. Tsuchiya, Y. Ishida and A. Kameyama, *Polym. Chem.*, 2017, **8**, 2516–2527.
55 Y. Tada, H. Yoshida, Y. Ishida, T. Hirai, J. K. Bosworth, E. Dobisz, R. Ruiz, M. Takenaka, T. Hayakawa and H. Hasegawa, *Macromolecules*, 2012, **45**, 292–304.
56 Y. Ishida, T. Hirai, R. Goseki, M. Tokita, M. A. Kakimoto and T. Hayakawa, *J. Polym. Sci., Part A: Polym. Chem.*, 2011, **49**, 2653–2664.
57 D. B. Cordes, P. D. Lickiss and F. Rataboul, *Chem. Rev.*, 2010, **110**, 2081–2173.
58 W.-A. Zhang and A. H. E. Müller, *Prog. Polym. Sci.*, 2013, **38**, 1121–1162.
59 L. X. Yang, Z. Z. Tian, X. Y. Zhang, X. Y. Wu, Y. Z. Wu, Y. A. Wang, D. D. Peng, S. F. Wang, H. Wu and Z. Y. Jiang, *J. Membr. Sci.*, 2017, **543**, 69.
60 T. Kamitani, A. Ishida, H. Imoto and K. Naka, *Polym. J.*, 2022, **54**, 161–167.
61 A. Nunns, J. Gwyther and I. Manners, *Polymer*, 2013, **54**, 1269–1284.
62 J. G. Son, K. W. Gotrik and C. A. Ross, *ACS Macro Lett.*, 2012, **1**, 1279–1284.
63 Y. Ni, R. Rulkens and I. Manners, *J. Am. Chem. Soc.*, 1996, **118**, 4102–4114.
64 W. C. Chen and S. W. Kuo, *Macromolecules*, 2018, **51**(23), 9602–9612.
65 Y. T. Liao, Y. C. Lin and S. W. Kuo, *Macromolecules*, 2017, **50**, 5739–5747.
66 A. Ullah, S. Ullah, G. S. Khan, S. M. Shah, Z. Hussain, S. Muhammad, M. Siddiq and H. Hussain, *Eur. Polym. J.*, 2016, **75**, 67–92.
67 W. B. Zhang, X. Yu, C. L. Wang, H. J. Sun, I. F. Hsieh, Y. Li, X. H. Dong, K. Yue, R. Van Horn and S. Z. D. Cheng, *Macromolecules*, 2014, **47**, 1221–1239.
68 G. K. Sethi, S. Chakraborty, C. Zhu, E. Schaible, I. Villaluenga and N. P. Balsara, *Gaint*, 2021, **6**, 100055.
69 H. Zhou, Q. Ye and J. Xu, *Mater. Chem. Front.*, 2017, **1**, 212–230.
70 Q. Ye, H. Zhou and J. Xu, *Chem. – Asian J.*, 2016, **11**, 1322–1337.
71 Y. Du and H. Liu, *Dalton Trans.*, 2020, **49**, 5396.
72 M. Chen, Y. Zhang, Q. Xie, W. Zhang, X. Pan, P. Gu, H. Zhou, Y. Gao, A. Walther and X. Fan, *ACS Biomater. Sci. Eng.*, 2019, **5**, 4612–4623.
73 L. Fan, X. Wang and D. Wu, *Chin. J. Chem.*, 2021, **39**, 757–774.
74 A. Uner, E. Doganci, M. A. Tasdelen, F. Yilmaz and A. G. Gürek, *Polym. Int.*, 2017, **66**, 1610–1616.
75 J. T. Weng, T. F. Yeh, A. Z. Samuel, Y. F. Huang, J. H. Sie, K. Y. Wu, C. H. Peng, H. O. Hamaguchi and C. L. Wang, *Nanoscale*, 2018, **10**, 3509–3517.
76 H. He, S. Chen, X. Tong, Z. An, M. Ma, X. Wang and X. Wang, *Langmuir*, 2017, **33**, 13332–13342.
77 X. Fan, M. Cao, X. Zhang and Z. Li, *Mater. Sci. Eng., C*, 2017, **76**, 211–216.
78 H. Chi, M. Wang, Y. Xiao, F. Wang and K. S. Joshy, *Molecules*, 2018, **23**, 2481.
79 X. Zhang, S. Zhao, S. W. Kuo, W. C. Chen, M. G. Mohamed and Z. Xin, *Polymer*, 2021, **220**, 123574.
80 H. K. Lin and Y. L. Liu, *Macromol. Rapid Commun.*, 2017, **38**, 1700051.
81 X. Y. Yan, Q. Y. Guo, X. Y. Liu, Y. Wang, J. Wang, Z. Su, J. Huang, F. Bian, H. Lin, M. Haung, Z. Lin, T. Liu, Y. Liu and S. Z. D. Zheng, *J. Am. Chem. Soc.*, 2021, **143**, 21613–21621.
82 H. Shi, J. Yang, M. You, Z. Li and C. He, *ACS Mater. Lett.*, 2020, **2**, 296–316.
83 W. Zhang, K. Gu, P. Hou, X. Lyu, H. Pan, Z. Shen and X. Fan, *Soft Matter*, 2018, **14**, 6774.
84 Y. Shao, S. Yang and W. B. Zhang, *Chem. – Eur. J.*, 2020, **26**, 2985–2992.
85 C. Y. Yu and S. W. Kuo, *Ind. Eng. Chem. Res.*, 2018, **57**, 2546–2559.
86 M. G. Mohamed and S. W. Kuo, *Polymers*, 2019, **11**, 26.
87 M. G. Mohamed, T. H. Mansoure, Y. Takashi, M. M. Samy, T. Chen and S. W. Kuo, *Microporous Mesoporous Mater.*, 2021, **328**, 111505.
88 M. G. Mohamed, W. C. Chen, A. F. M. EL-Mahdy and S. W. Kuo, *J. Polym. Res.*, 2021, **28**, 219.
89 Z. Su, R. Zhang, X. Y. Yan, Q. Y. Guo, J. Haung, W. Shan, Y. Liu, T. Liu, M. Huang and S. Z. D. Cheng, *Prog. Polym. Sci.*, 2020, **103**, 101230.
90 M. G. Mohamed, M. Y. Tsai, C. F. Wang, C. F. Huang, M. Danko, L. Dai, T. Chen and S. W. Kuo, *Polymers*, 2021, **13**, 221.
91 X. Zhang, S. Zhao, M. G. Mohamed, S. W. Kuo and Z. Xin, *J. Mater. Sci.*, 2020, **55**, 14642–14655.

92 M. G. Mohamed and S. W. Kuo, *Macromol. Chem. Phys.*, 2019, **220**, 1800306.
93 S. W. Kuo, *J. Polym. Res.*, 2022, **29**, 69.
94 S. W. Kuo and F. C. Chang, *Prog. Polym. Sci.*, 2011, **36**, 1649–1696.
95 X. Zhang, W. Wei and H. Xiong, *Macromolecules*, 2022, **55**, 3637–3649.
96 C. M. Leu, Y. T. Chang and K. H. Wei, *Macromolecules*, 2003, **36**, 9122–9127.
97 Y. T. Xu, J. F. Chen, J. M. Huang, J. Cao, J. F. Gerard and L. Z. Dai, *High Perform. Polym.*, 2017, **29**, 1148–1157.
98 J. Wu, X. Y. Song, L. T. Zeng and J. F. Xing, *Colloid Polym. Sci.*, 2016, **294**, 1315–1324.
99 X. Qiang, F. Chen, M. Y. Ma and X. B. Hou, *J. Appl. Polym. Sci.*, 2014, **131**, 40652–40660.
100 W. Zhang and A. H. E. Müller, *Polymer*, 2010, **51**, 2133–2139.
101 C. Wang, L. Zhou, Q. Du, T. Shan, K. Zheng, J. He, H. He, S. Chen and X. Wang, *Polym. Int.*, 2022, **71**, 379–392, DOI: **10.1002/pi.6317**.
102 J. Duszczak, K. Mitula, R. Januszewski, P. Zak, B. Dudziec and B. Marciniec, *ChemCatChem*, 2019, **11**, 1086–1091.
103 J. C. Wang, W. N. Du, Z. T. Zhang, W. Y. Gao and Z. J. Li, *J. Appl. Polym. Sci.*, 2021, **138**, 51242.
104 C. F. Huang, S. W. Kuo, F. J. Lin, W. J. Huang, C. F. Wang, W. Y. Chen and F. C. Chang, *Macromolecules*, 2006, **39**, 300–308.
105 S. W. Kuo, H. F. Lee, W. J. Huang, K. U. Jeong and F. C. Chang, *Macromolecules*, 2009, **42**, 1619–1626.
106 S. W. Kuo and H. T. Tsai, *Polymer*, 2010, **51**, 5695–5704.
107 G. Cardoen and E. B. Coughlin, *Macromolecules*, 2004, **37**, 5123–5126.
108 X. Yu, S. Zhong, X. Li, Y. Tu, S. Yang, R. M. Van Horn, C. Ni, D. J. Pochan, R. P. Quirk, C. Wesdemiotis, W. B. Zhang and S. Z. D. Cheng, *J. Am. Chem. Soc.*, 2010, **132**, 16741–16744.
109 X. Yu, K. Yue, L. F. Hsieh, Y. Li, X. H. Dong, C. Liu, Y. Xin, H. F. Wang, A. C. Shř, G. R. Newkome, R. M. Ho, E. Q. Chen, W. B. Zhang and S. Z. D. Cheng, *Proc. Natl. Acad. Sci. U. S. A.*, 2013, **110**, 10078–10083.
110 W. J. Wang, X. Xu, Y. Shao, J. W. Liao, H. X. Jian, B. Xue and S. G. Yang, *Chin. J. Chem.*, 2022, **40**, 556–566.
111 M. Huang, C.-H. Hsu, J. Wang, S. Mei, X. Dong, Y. Li, M. Li, H. Liu, W. Zhang, T. Aida, W.-B. Zhang, K. Yue and S. Z. D. Cheng, *Science*, 2015, **348**, 424–428.
112 Z. Su, C. H. Hsu, Z. Gong, X. Feng, J. Huang, R. Zhang, Y. Wang, J. Mao, C. Wesdemiotis, T. Li, S. Seifert, W. Zhang, T. Aida, M. Huang and S. Z. D. Cheng, *Nat. Chem.*, 2019, **11**, 899–905.
113 X. Feng, G. Liu, D. Guo, K. Lang, R. Zhang, J. Huang, Z. Su, Y. Li, M. Huang, T. Li and S. Z. D. Cheng, *ACS Macro Lett.*, 2019, **8**, 875–881.
114 K. Yue, M. Huang, R. L. Marson, J. He, J. Huang, Z. Zhou, J. Wang, C. Liu, X. Yan, K. Wu, Z. Guo, H. Liu, W. Zhang, P. Ni, C. Wesdemiotis, W.-B. Zhang, S. C. Glotzer and S. Z. D. Cheng, *Proc. Natl. Acad. Sci. U. S. A.*, 2016, **113**, 14195–14200.
115 W. Zhang, W. Shan, S. Zhang, Y. Liu, H. Su, J. Luo, Y. Xia, T. Li, C. Wesdemiotis, T. Liu, H. Cui, Y. Li and S. Z. D. Cheng, *Chem. Commun.*, 2019, **55**, 636–639.
116 F. Feng, D. Guo, Y. Shao, X. Yan, K. Yue, Z. Pan, X. Li, D. Xiao, L. Jin, W. B. Zhang and H. Liu, *Chem. Sci.*, 2021, **12**, 5216–5223.
117 W. Zhang, Y. Chu, G. Mu, S. A. Eghtesadi, Y. Liu, Z. Zhou, X. Lu, M. A. Kashfipour, R. S. Lillard, K. Yue, T. Liu and S. Z. D. Cheng, *Macromolecules*, 2017, **50**, 5042–5050.
118 T. Liu, H. Zhao, J. Li, W. Zheng and L. Wang, *Corros. Sci.*, 2020, **168**, 108555.
119 Q. Y. Guo, X. Y. Yan, W. Zhang, X. H. Li, Y. Xu, S. Dai, Y. Liu, B. X. Zhang, X. Feng, J. Yin, D. Han, J. Huang, Z. Su, T. Liu, M. Huang, C. H. Hsu and S. Z. D. Cheng, *J. Am. Chem. Soc.*, 2021, **143**, 12935–12942.
120 F. Feng, Y. Shao, W. Wu, X. Li, C. Hong, L. Jin, K. Yue, W. B. Zhang and H. Liu, *Macromolecules*, 2021, **54**, 11093–11100.
121 Y. Sun, J. Kim and K. T. Kim, *RSC Adv.*, 2019, **9**, 25423.
122 H. M. Lin, S. Y. Wu, P. Y. Huang, C. F. Huang, S. W. Kuo and F. C. Chang, *Macromol. Rapid Commun.*, 2006, **27**, 1550–1555.
123 H. Xu, S. W. Kuo, J. S. Lee and F. C. Chang, *Polymer*, 2002, **43**, 5117–5124.
124 H. Xu, S. W. Kuo, J. S. Lee and F. C. Chang, *Macromolecules*, 2002, **35**, 8788–8793.
125 C. W. Chiou, Y. C. Lin, L. Wang, C. Hirano, Y. Suzuki, T. Hayakawa and S. W. Kuo, *Polymers*, 2014, **6**, 926–948.
126 Y. C. Lin and S. W. Kuo, *Polym. Chem.*, 2012, **3**, 162–171.
127 P. L. Cortes, T. B. Huq and J. L. Vivero-Escoto, *Molecules*, 2021, **26**, 6453.
128 F. Dong, L. Lu and C. S. Ha, *Macromol. Chem. Phys.*, 2019, **220**, 1800324.
129 B. Zhao, H. Mei, H. Wang, L. Li and S. Zheng, *ACS Appl. Polym. Mater.*, 2022, **4**, 509–520.
130 Y. Ma, H. Wu and Y. Shen, *J. Mater. Sci.*, 2022, **57**, 7791–7803.
131 A. Takahashi, T. Okada, K. Nakano, Y. Ishida and A. Kameyama, *Polym. J.*, 2021, **53**, 1213–1222.
132 J. Pyun, K. Matyjaszewski, J. Wu, G. M. Kim, S. B. Chun and P. T. Mather, *Polymer*, 2003, **44**, 2739–2750.
133 T. Hirai, M. Leolukman, S. Jin, R. Goseki, Y. Ishida, M. Kakimoto, T. Hayakawa, M. Ree and P. Gopalan, *Macromolecules*, 2009, **42**, 8835–8843.
134 C. W. Chiou, Y. C. Lin, L. Wang, R. Maeda, T. Hayakawa and S. W. Kuo, *Macromolecules*, 2014, **47**(24), 8709–8721.
135 Y. C. Lin and S. W. Kuo, *Polym. Chem.*, 2012, **3**, 882–891.
136 B. Zhao, S. Xu and S. Zheng, *Polym. Chem.*, 2019, **10**, 2424–2435.
137 J. Jin, M. Tang, Z. Zhang, K. Zhou, Y. Gao, Z. G. Zheng and W. Zhang, *Polym. Chem.*, 2018, **9**, 2101–2108.
138 Y. Xu, K. He, H. Wang, M. Li, T. Shen, X. Liu, C. Yuan and L. Dai, *Micromachines*, 2018, **9**, 258.
139 C. G. Chae, Y. G. Yu, H. B. Seo, M. J. Kim, M. Y. L. N. Kishore and J. S. Lee, *Polym. Chem.*, 2018, **9**, 5179–5189.
140 C. S. Meng, Y. K. Yan and W. Wang, *Polym. Chem.*, 2017, **8**, 6824–6833.

 

141 J. Liang, L. He, Y. Zuo, Z. Chen and T. Peng, *Soft Matter*, 2018, **14**, 5235–5245.
142 Z. Zhang, L. Hong, Y. Gao and W. Zhang, *Polym. Chem.*, 2014, **5**, 4534–4541.
143 X. M. Wang, Q. Y. Guo, S. Y. Han, J. Y. Wang, D. Han, Q. Fu and W. B. Zhang, *Chem. – Eur. J.*, 2015, **21**, 15246–15255.
144 Z. Liu, Z. Yang, X. Chen, R. Tan, G. Li, Z. Gan, Y. Shao, J. He, Z. Zhang, W. Li, W. B. Zhang and X. H. Dong, *JACS Au*, 2021, **1**, 79–86.
145 Y. Shao, H. Yin, X. M. Wang, S. Y. Han, X. Yan, J. Xu, J. He, P. Ni and W. B. Zhang, *Polym. Chem.*, 2016, **7**, 2381–2388.
146 X. M. Wang, Y. Shao, J. Xu, X. Jin, R. H. Shen, P. F. Jin, D. W. Shen, J. Wang, W. Li, J. He, P. Ni and W. B. Zhang, *Macromolecules*, 2017, **50**, 3943–3953.
147 W. C. Chen, Y. H. Tsao, C.-F. Wang, C. F. Huang, L. Dai, T. Chen and S. W. Kuo, *Polymers*, 2020, **12**, 465.
148 W. C. Chen, Y. T. Liu and S. W. Kuo, *Macromol. Rapid Commun.*, 2021, **42**, 2170061.
149 W. C. Chen, Y. T. Liu and S. W. Kuo, *Polymers*, 2020, **12**, 2151.
150 Y. Wang, J. Huang, X. Y. Yan, H. Lei, X. Y. Liu, Q. Y. Guo, Y. Liu, T. Liu, M. Huang, F. Bian, Z. Su and S. Z. D. Cheng, *Angew. Chem., Int. Ed.*, 2022, **61**, e202200637.
151 Y. Liu, T. Liu, X. Y. Yan, Q. Y. Guo, H. Lei, Z. Huang, R. Zhang, Y. Wang, J. Wang, F. Liu, F. G. Bian, E. W. Meijer, T. Aida, M. Huang and S. Z. D. Cheng, *Proc. Natl. Acad. Sci. U. S. A.*, 2022, **119**, e2115304119.
152 Y. Shao, D. Han, X. Yan, B. Hou, Y. Li, J. He, Q. Fu and W. B. Zhang, *Chin. J. Chem.*, 2021, **39**, 3261–3268.
153 H. R. Abuzeid, A. F. M. EL-Mahdy and S. W. Kuo, *Giant*, 2021, **6**, 100054.
154 M. G. Mohamed, S. U. Sharma, N. Y. Liu, T. H. Mansoure, M. M. Samy, S. V. Chaganti, Y. L. Chang, J. T. Lee and S. W. Kuo, *Int. J. Mol. Sci.*, 2022, **23**, 3174.
155 M. G. Mohamed, T. H. Mansoure, M. M. Samy, Y. Takashi, A. A. K. Mohammed, T. Ahamad, S. M. Alshehri, J. Kim, B. M. Matsagar, K. C. W. Wu and S. W. Kuo, *Molecules*, 2022, **27**, 2025.
156 M. G. Mohamed, S. V. Chaganti, M. S. Li, M. M. Samy, S. U. Sharma, J. T. Lee, M. H. Elsayed, H. H. Chou and S. W. Kuo, *ACS Appl. Energy Mater.*, 2022, **5**, 6422–6452.
157 M. G. Mohamed, M. M. Samy, T. H. Mansoure, C. J. Li, W. C. Li, J. H. Chen, K. Zhang and S. W. Kuo, *Int. J. Mol. Sci.*, 2022, **23**, 347.
158 M. G. Mohamed, A. F. M. EL-Mahdy, M. G. Kotp and S. W. Kuo, *Mater. Adv.*, 2022, **3**, 707–733.
159 M. M. Samy, M. G. Mohamed, T. H. Mansoure, T. S. Meng, M. A. R. Khan, C. C. Liaw and S. W. Kuo, *J. Taiwan Inst. Chem. Eng.*, 2022, **132**, 104110.
160 A. M. Elewa, A. F. M. EL-Mahdy, M. H. Elsayed, M. G. Mohamed, S. W. Kuo and H. H. Chou, *Chem. Eng. J.*, 2021, **421**, 129825.
161 M. G. Mohamed, T. C. Chen and S. W. Kuo, *Macromolecules*, 2021, **54**, 5866–5877.
162 M. G. Mohamed, M. H. Elsayed, A. M. Elewa, A. F. M. EL-Mahdy, C. H. Yang, A. A. K. Mohammed, H. H. Chou and S. W. Kuo, *Catal. Sci. Technol.*, 2021, **11**, 2229–2241.
163 M. G. Mohamed, C. C. Lee, A. F. M. EL-Mahdy, J. Lüder, M. H. Yu, Z. Li, Z. Zhu, C. C. Chueh and S. W. Kuo, *J. Mater. Chem. A*, 2020, **8**, 11448–11459.
164 Z. Liu, S. Ma, L. Chen, J. Xu, J. Ou and M. Ye, *Mater. Chem. Front.*, 2019, **3**, 851–859.
165 M. M. Samy, I. M. A. Mekhemer, M. G. Mohamed, M. H. Elsayed, K. H. Lin, Y. K. Chen, T. L. Wu, H. H. Chou and S. W. Kuo, *Chem. Eng. J.*, 2022, **446**, 137158.
166 R. Majumdar, C. Wannasiri, M. Sukwattanasinitt and V. Ervithayasuporn, *Polym. Chem.*, 2021, **12**, 3391–3412.
167 M. G. Mohamed, S. V. Chaganti, M. S. Li, M. M. Samy, S. U. Sharma, J. T. Lee, M. H. Elsayed, H. H. Chou and S. W. Kuo, *ACS Appl. Energy Mater.*, 2022, **5**, 6442–6452.
168 A. Shimojima and K. Kuroda, *Molecules*, 2020, **25**, 524.
169 Y. C. Wu and S. W. Kuo, *Polymer*, 2010, **51**, 3948–3955.
170 W. H. Hu, K. W. Huang and S. W. Kuo, *Polym. Chem.*, 2012, **3**, 1546–1554.
171 W. H. Hu, K. W. Huang, C. W. Chiou and S. W. Kuo, *Macromolecules*, 2012, **45**, 9020–9028.
172 J. H. Wang, O. Altukhov, C. C. Cheng, F. C. Chang and S. W. Kuo, *Soft Matter*, 2013, **9**, 5196–5206.
173 Y. Xue, D. Huang, X. Wang and C. Zhang, *Polymers*, 2022, **14**, 1695.
174 E. Doganci, M. A. Tasdelen and F. Yilmaz, *Macromol. Chem. Phys.*, 2015, **216**, 1823–1830.
175 L. Jia, J. Ma, D. Gao, W. R. T. Tait and L. Sun, *J. Hazard. Mater.*, 2019, **361**, 305–311.
176 P. F. Jin, Y. Shao, G. Z. Yin, S. Yang, J. He, P. Ni and W. B. Zhang, *Macromolecules*, 2018, **51**, 419–427.
177 P. Zhang, Z. Zhang, X. Jiang, L. Rui, Y. Gao and W. Zhang, *Polymer*, 2017, **118**, 268–279.
178 K. Bhattacharya, S. L. Banerjee, M. Kundu, M. Mandal and N. K. Singha, *Mater. Sci. Eng., C*, 2020, **116**, 111210.
179 X. Zhou, X. Fan and C. He, *Macromolecules*, 2016, **49**, 4236–4244.
180 C. H. Lu, J. H. Wang, F. C. Chang and S. W. Kuo, *Macromol. Chem. Phys.*, 2010, **211**, 1339–1347.
181 G. Li, Z. Gan, Y. Liu, S. Wang, Q. Y. Guo, Z. Liu, R. Tan, D. Zhou, D. Kong, T. Wen and X. H. Dong, *ACS Nano*, 2020, **14**, 13816–13823.